Adaptive substitutions underlying cardiac glycoside insensitivity in insects exhibit epistasis *in vivo*

Andrew M. Taverner[1], Lu Yang[2], Zackery J. Barile[3,4], Becky Lin[3,4], Julie Peng[1], Ana Pinharanda[5], Arya Rao[5], Bartholomew P. Roland[3,4], Aaron D. Talsma[3,4], Daniel Wei[3,4], Georg Petschenka[6], Michael J. Palladino[3,4,*] and Peter Andolfatto[5,*]

1. Lewis-Sigler Institute for Integrative Genomics, Princeton University, Princeton, NJ 08544.
2. Dept. of Ecology and Evolutionary Biology, Princeton University, Princeton, NJ 08544.
3. Dept. of Pharmacology and Chemical Biology, University of Pittsburgh, Pittsburgh, PA 15261.
4. Pittsburgh Institute for Neurodegenerative Diseases (PIND), University of Pittsburgh School of Medicine, Pittsburgh, PA 15261.
5. Department of Biological Sciences, Columbia University, New York, NY 10027
6. Institute for Insect Biotechnology, Justus-Liebig-Universität Gießen, Hesse, Germany

*Correspondence: Peter Andolfatto, pa2543@columbia.edu, Michael Palladino, mp44@upitt.edu

Short title: Epistasis among adaptive substitutions *in vivo*

Abstract

Predicting how species will respond to selection pressures requires understanding the factors that constrain their evolution. We use genome engineering of *Drosophila* to investigate constraints on the repeated evolution of unrelated herbivorous insects to toxic cardiac glycosides, which primarily occurs via a small subset of possible functionally-relevant substitutions to Na^+,K^+-ATPase. Surprisingly, we find that frequently observed adaptive substitutions at two sites, 111 and 122, are lethal when homozygous and adult heterozygotes exhibit dominant neural dysfunction. We identify a phylogenetically correlated substitution, A119S, that partially ameliorates the deleterious effects of substitutions at 111 and 122. Despite contributing little to cardiac glycoside-insensitivity *in vitro*, A119S, like substitutions at 111 and 122, substantially increases adult survivorship upon cardiac glycoside exposure. Our results demonstrate the importance of epistasis in constraining adaptive paths. Moreover, by revealing distinct effects of substitutions *in vitro* and *in vivo*, our results underscore the importance of evaluating the fitness of adaptive substitutions and their interactions in whole organisms.

Introduction

Understanding the factors that limit the rate of adaptation is central to our ability to forecast future adaptive evolutionary trajectories and predict the timescales over which these changes are expected to occur (Stern 2011; Losos 2017; Morris et al. 2018). In particular, considerable uncertainty surrounds the relative importance of the availability of adaptive mutations, pleiotropy and epistasis in constraining adaptive paths (Stern 2011; Storz 2018). One fruitful approach to addressing this question has been to examine repeated bouts of adaptation in microbial systems subject to a common selective pressure and identical starting conditions (Jerison and Desai 2015). Unfortunately, such approaches still have limited utility in multicellular eukaryotes and likely don't reveal the full range of constraints operating in nature. An alternative and analogous approach is to examine evolutionary patterns in large, naturally occurring assemblages of species exhibiting parallel adaptations in response to a common selective pressure (Liu et al. 2010; Meyer et al. 2018; Zhen et al. 2012; Dobler et al. 2012; Christin et al. 2007). Evolutionary studies of parallelisms are a powerful complementary approach to deducing the factors constraining the adaptation (Stern 2013). A well-known example of parallel adaptations is the ability of numerous animals to acquire toxins from their environments and sequester them for use in defense against predators (Brodie 2009; Erb and Robert 2016).

Here, we focus on a large group of herbivorous insects with a broad phylogenetic distribution that have independently specialized on toxic host plants (Dobler et al. 2011). In addition to other defenses against herbivory, the Apocynaceae and other plant species produce a class of toxic secondary compounds called cardiac glycosides (CGs). CGs are highly toxic to animals because they are potent inhibitors of Na^+,K^+-ATPase (NKA), a ubiquitously expressed enzyme needed in a variety of cellular processes in animals, including neural signal transduction, muscle contraction, and osmoregulation (Lingrel 2010). Mutations to NKA in invertebrates are typically homozygous lethal and associated with defects in locomotion, neuron development and neural homeostasis (Ashmore et al. 2009). In humans, loss-of-function mutations in NKA have been associated with several rare disorders such as dystonia, parkinsonism and hemiplegic migraines (Bøttger et al. 2012). Despite their toxicity, NKAs have long been targeted with CG-based drugs to treat common conditions such as congestive heart failure and cardiac arrhythmias (Schoner 2002).

Insensitivity to CGs in insects can evolve via several mechanisms including modification of the CG-binding domain of NKA (i.e. target-site insensitivity), restriction of NKA expression to neurons (Petschenka et al. 2013b), the deployment of proteins that ameliorate the toxic effects of CGs (Torrie et al. 2004; Petschenka et al. 2013b) and other physiological factors (Vaughan and Jungreis 1977). Despite this wide variety of potential paths to CG-insensitivity, the evolution of insensitivity in most CG-adapted insects is due, at least in part, to target-site insensitivity. Indeed, in most cases, diet specialization on CG-containing hostplants has been accompanied by recurrent adaptive amino acid substitutions to the CG-binding domain of the alpha-subunit of NKA, ATPα1 (Zhen et al. 2012; Dobler et al. 2012; Yang et al. 2019). Previous studies have identified up to 35 sites in ATPα1 at which substitutions could contribute to CG-insensitivity (reviewed in Zhen et al. 2012). However, CG-insensitivity of ATPα1 most often arises via a highly similar pattern of substitution at two sites (111 and 122, **Figure 1A**): as an illustration, a survey of 28 CG-adapted insects revealed that 30 of 63 amino acid substitutions

observed at sites implicated in CG-sensitivity in ATPα1 occur at sites 111 and 122 (Yang et al. 2019). Sites 111 and 122 have also been identified as targets of positive selection in CG-adapted insects using statistical phylogenetic methods (Yang et al. 2019). Understanding why these two sites, in particular, are so often employed requires a characterization of the effects of these substitutions, individually and in combination, on organismal phenotypes and fitness.

To explain the frequent reuse of sites 111 and 122, it has been speculated that substitutions at most alternative sites may be associated with negative pleiotropic effects, that is, have deleterious effects on another aspect of phenotype and fitness (Zhen et al. 2012). Support for this hypothesis comes from the fact that multiple insect species specializing on CG-containing host-plants have independently duplicated and neofunctionalized ATPα1. In all cases examined to date, species with two or more copies retain one minimally altered copy that is more highly expressed in nervous tissue, and have evolved one or more insensitive copies that are more highly expressed in the gut, the site of absorption of CGs (Zhen et al. 2012; Yang et al. 2019). Further support for negative pleiotropic effects is provided by the expression of engineered ATPα1 constructs in cell lines, suggesting that some duplicate-specific CG-insensitivity substitutions appear to reduce NKA activity (Dalla and Dobler 2016). Based on these findings, the frequent parallel substitutions observed at sites 111 and 122 in specialists lacking duplicate ATPα1 copies plausibly reflect the fact that substitutions at these sites are minimally pleiotropic.

Common substitutions at positions 111 and 122 exhibit negative pleiotropic effects.

To test the idea that substitutions at positions 111 and 122 lack strong negative pleiotropic effects, we used the transgenesis toolkit of *Drosophila melanogaster*, a generalist insect that harbors a single ubiquitously expressed copy of a CG-sensitive form of ATPα1. This sensitive form of ATPα1 is the presumptive ancestral state for many potential CG-adapted insects. We focus on several substitutions at sites 111 and 122 (notably Q111V, Q111T, N122H, **Figure 1A**) have been directly implicated in CG-insensitivity in functional experiments (reviewed in Zhen et al. 2012). By engineering amino acid substitutions into a single *D. melanogaster* background, we ensure that fitness differences observed among lines are caused by the substitution and not confounded by unknown variation in the genomic background. In addition, we can rule out compensatory changes elsewhere in the genome, or evolved changes in physiology, which are concerns in multi-generation population-level experimental evolution studies. Importantly, by testing substitutions *in vivo*, we can evaluate their functional effects at multiple phenotypic levels, from the biochemistry of enzyme inhibition to behavior and fitness. We generated six lines that carry substitutions at these two sites of the endogenous ATPα1 locus individually (Q111L, Q111V, Q111T, N122H) and in combination (Q111V+N122H, Q111T+N122H) (see Methods). For comparison, we also created three lines in which we introduced two rare, copy-specific substitutions (C104Y and N122Y and C104Y+N122Y, **Figure 1A**) for which we did not have *a priori* expectations about pleiotropic fitness effects. C104Y is known to confer some degree of insensitivity to CGs, and both C104Y and N122Y occur on a neofunctionalised copy of ATPα1 in the milkweed weevil (Zhen et al. 2012). An additional control line carrying the wild-type *D. melanogaster* allele was generated using the same approach.

Based on the repeated use of substitutions at positions 111 and 122, we expected these would confer ATPα1 with some degree of insensitivity to CGs and be associated with either no

or mild negative pleiotropic effects on fitness. To our surprise, however, each of the nine lines exhibit severely reduced fitness, behaving effectively as recessive lethals. To identify the developmental stage at which lethality occurs, we evaluated hatchability (i.e. the proportion of homozygous larva per embyro) and the probability of individuals surviving to pupae and adults (**Figure 1B**). Severe fitness deficits for most engineered substitution lines were apparent as early as the larval hatching stage. Still, for most engineered mutant lines, greater than 50% of individuals hatch into the first instar. Q111V homozygotes exhibit particularly high probabilities of survival until the pupal stage. Nonetheless, survivorship of individuals to adulthood for all lines is close to zero.

The substitution A119S rescues lethality of substitutions at sites 111 and 122.

The unexpected deleterious effects of common substitutions at sites 111 and 122 raises the question of how insects with sensitive ATPα1 isoforms, spanning a broad phylogenetic distribution, can evolve insensitivity to CGs via substitutions to one or both of these sites. An important clue is provided by the observation that *D. subobscura*, a European relative of *D. melanogaster,* carries haplotypes resembling those that we engineered into *D. melanogaster*, including the ancestral (QN) and derived states (QH and VH) at sites 111 and 122, respectively (Pegueroles et al. 2016), and yet are viable. Full length coding sequences for *D. subobscura* (**Methods**) and the closely related sister species *D. guanche* (Puerma et al. 2018) reveal that 19 amino acid substitutions distinguish the *D. melanogaster* ATPα1 from the ancestral *D. subobscura* protein. We hypothesized that one or more of these substitutions ameliorates the deleterious effects of substitutions at positions 111 and 122.

Using a multiple sequence alignment that includes 161 CG-adapted insects and outgroup species surveyed from six insect orders (**Figures S1 and S2, Figure 1A** shows a subset of these taxa), we applied the software BayesTraits (Pagel and Meade 2006) to evaluate the evidence for correlated evolution between sites 111 and 122 and all other variant sites in the protein (**Methods**). Of the divergent sites between *D. melanogaster* and *D. subobscura*, only one site (119) is among those having the strongest phylogenetic correlations with both sites 111 and 122 (top 5% of 270 sites) (**Figure 1C, Figure S3**). A substitution at 119 is observed in 90% of the cases in which there is a substitution at 111 and 100% of the cases in which there is a substitution at site 122. *D. melanogaster* retains the ancestral Alanine at this site, whereas the *D. subobscura* and closely-related species harbor a derived Serine substitution.

Though site 119 is not among sites known to affect CG-sensitivity (Zhen et al. 2012), previous work identified it as one of four sites in the protein that underlie a CG-association/dissociation rate difference distinguishing human ATP1A1 and ATP1A2 isoforms (Crambert et al. 2004). Considering the orientation of the amino-acid side chain of site 119 with respect to a bound CG (**Figure S4**), it is unlikely that it plays a direct role in CG binding. Nonetheless, due to its physical proximity to sites 111 and 122 and the evidence for correlated evolution with these sites, we hypothesized that the A119S substitution may compensate for the deleterious effects of substitutions at positions 111 and 122. To test this hypothesis, we generated a second series of substitution lines that include A119S in isolation, and A119S paired with four substitutions at sites 111 and 122 (i.e. Q111L+A119S, Q111V+A119S, Q111T+A119S and A119S+N122H, **Figure 1D**). Embryos homozygous for A119S, with and without substitutions at 111 and 122, have levels of hatchability and survival that are close to

wild-type levels. Remarkably, we find that A119S rescues the lethality associated with homozygosity for all four substitutions with which we paired it (i.e. compare **Figure 1D** with **Figure 1B**). These results establish the existence of epistatic fitness interactions between A119S and multiple substitutions at both 111 and 122.

A119S rescues enzyme dysfunction associated with substitutions at sites 111 and 122.

To gain insight into the functional basis of the fitness interaction between A119S and substitutions at sites 111 and 122 at the level of NKA function, we carried out a series enzyme inhibition assays (**Figure 2, Figure S5**). For lines that are heterozygous for CG-insensitivity substitutions, Mut/+, we expect to see biphasic inhibition curves reflecting the equilibrium dissociation constants (K_d) corresponding to the wild-type (+) and mutant (Mut) forms of the enzyme, respectively. Comparing biphasic curves for heterozygotes allows us to directly compare inhibition profiles for homozygous-inviable substitutions at positions at 111 and 122 alone and in combination with A119S. **Figure 2A** details the analysis of the A119S and N122H substitutions in this context. The inhibition curve for A119S/+ appears to be monophasic suggesting that A119S alone has little effect on CG inhibition of NKA. In contrast, the inhibition curve for N122H/+ heterozygotes is biphasic. However, while this implies that N122H substantially increases CG-insensitivity ($IC_{50,2}$ = 6.6e-6), the contribution of the N122H form to the total CG-inhibitable activity in heterozygotes is estimated to be less than half that of the wild-type form (f = 0.18, 95% CI 0.14 - 0.24). An analysis of allele-specific expression of N122H/+ indicates close to equal mRNA levels for the two alleles (**Figure S6**), suggesting that the differences in activity are not due to differences at the level of gene expression. Thus, despite conferring CG-insensitivity, the N122H substitution likely encodes a functionally-impaired enzyme.

In contrast to N122H/+, N122H+A119S/+ heterozygotes produce a strongly biphasic inhibition curve, with a two-fold higher estimated $IC_{50,2}$ = 1.9e-5 and comparable levels of activity to that of the wild-type form (f =0.53, 95% CI 0.47-0.56, **Figure 2A)**. Similar results were obtained in comparisons of Q111V and Q111V+A119S (**Figure S5**). We estimate the level of CG-insensitivity conferred by Q111L, Q111V, Q111T and N122H, in the presence of A119S, to be 7, 11, 28 and 178-fold greater than the wild-type form of the enzyme, respectively (**Figure 2B**). Our results demonstrate epistasis between substitutions at sites 119 and 111/122 at the level of enzyme function. Previous studies have demonstrated increased survival of cell lines expressing Q111V, N122H, and Q111T+Q111H (Dobler et al. 2012), and substantial insensitivity to CG-inhibition despite little effect on ATPase activity for N122H, Q111T+Q111H and Q111V+Q111H (Dalla et al. 2013; Dalla and Dobler 2016). Given that these substitutions were engineered on a *D. melanogaster* background lacking A119S, our results suggest such substitutions are likely to be associated with substantial enzyme dysfunction.

A119S rescues neural dysfunction associated with substitutions at sites 111 and 112 *in vivo*.

An advantage of functionally testing the effects of amino acid substitutions *in vivo*, as opposed to *in vitro*, is the ability to examine fitness-related phenotypes at multiple levels. We therefore considered the impact of substitutions, alone and in combination, on higher level fitness-related phenotypes including adult behavior in response to stress and survivorship of adult flies exposed to CGs.

NKA plays a central role in maintaining neuron action potentials and previous studies have documented short-term paralysis following mechanical overstimulation (aka "bang sensitivity") associated with mutations that reduce this enzyme's activity (Ganetzky and Wu 1982; Schubiger et al. 1994; Davis et al. 1995; Palladino et al. 2003). As such, we used the bang sensitivity phenotype as a proxy for proper neural function. Examining our panel of substitutions for these effects reveals all of the substitutions we engineered at sites 111 and 122, individually and in combination, exhibit dominant bang sensitivity phenotypes that are similar in severity to those of the loss-of-function deletion Δ2-6b (**Figure 3A, Figure S7**). In contrast, bang sensitivity phenotypes were indistinguishable from wild-type for all heterozygous substitutions at 111 and 122 in combination with A119S (**Figure 3A, Figure S8**). Interestingly, individuals homozygous for A119S, and substitutions at 111 and 122 in the presence of A119S, still exhibit obvious neural dysfunction relative to the wildtype (**Figure 3, Figure S8**). Thus, while A119S is itself associated with recessive pleiotropic effects, our results demonstrate some degree of positive epistasis between A119S and substitutions at sites 111 and 122 when considering the level of adult behavior.

Substitutions at sites 111, 119 and 122 increase adult survival upon exposure to CGs.

D. melanogaster do not normally consume CG-containing plants and consumption of CGs results in increased mortality (Groen et al. 2017). Given that substitutions at sites 111 and 122 decrease sensitivity to CG-inhibition of NKA, such substitutions should confer an advantage upon exposure of *D. melanogaster* to CGs. To test this hypothesis, we exposed adult animals to media containing the CG ouabain. While the wild-type strain suffers high levels of mortality upon CG exposure, the lines carrying substitutions at sites 111 and 122 in combination with A119S are all substantially less-sensitive (**Figure 4, Figure S9**). Notably, the survival probability of A119S+N122H (SH/+ and SH/SH) is indistinguishable from control treatments in exposures with up to 10 mM ouabain. Beyond confirming an association between insensitivity to CG-inhibition of enzyme activity *in vitro* and reduced sensitivity to CG-exposure *in vivo*, two additional important findings arise from these experiments. First, a substantial measure of insensitivity to CG-exposure is also conferred by A119S alone (S/+ and S/S exhibit ~8.5-fold and ~21-fold lower relative risk, respectively, than wild-type at 5 mM ouabain, **Figure 4**). Despite this, A119S alone has only a small effect on NKA sensitivity to CG-inhibition (**Figure 2**). Further, the substantially improved survival of heterozygous strains relative to the wild-type strain, including to some extent A119S/+, suggests that insensitivity to CG exposure is a partially dominant phenotype (**Figure 4, Figure S9**). Importantly, despite the lethal homozygous effects of Q111V and N122H individually (**Figure 1B**), the dominant effects of these substitutions on insensitivity to CG-exposure imply that they have the potential to confer a fitness advantage as heterozygotes in CG-rich environments.

Implications for the evolution of CG-insensitivity in insects.

Our findings carry important implications for how CG-insensitivity evolves in insects. At the onset of this study, we expected minimal negative pleiotropic effects associated with adaptive substitutions at sites 111 and 122, given their frequent parallel occurrence across insect orders (Zhen et al. 2012). Our findings that these substitutions are associated with negative pleiotropic effects at multiple levels (i.e. enzyme function, neural function and viability) reveals a more

complicated explanation. As we show, with few exceptions, adaptive substitutions conferring CG-insensitivity at sites 111 and 122 most often arise on a genetic background that includes a substitution at site 119, a site not previously implicated in CG-sensitivity. We further show that the most commonly observed substitution at sites 119, A119S, rescues the lethality associated with substitutions at sites 111 and 122, as well as their dominant effects on neural function. A second common substitution, A119N, appears independently in three insect orders and may act similarly (**Figure 1A**, **Figure S2**). Thus, the repeated use of specific substitutions does not mean that these changes unconditionally lack negative pleiotropic consequences and that their fitness advantage can depend critically on the background on which they arise.

To the extent that *D. melanogaster* represents a typical CG-sensitive species, it is clear that substitutions at positions 111 and 122 would not be permitted to fix in the species without being preceded by A119S or an equivalent permissive substitution. A119S was not detected in extensive mutagenesis screens (Zhen et al. 2012) and has only modest effects on CG-inhibition of NKA *in vitro* (**Figure 2**). Given these findings and its position and orientation in the NKA-ouabain co-crystal structure (**Figure S4**), one might assume that A119S is a neutral (or nearly-neutral) permissive substitution that renders some species candidates for the adaptation to CGs by chance. However, our ability to examine the effects of A119S, and interacting substitutions, in the context of whole animal phenotypes reveals a remarkably different picture. In particular, we show that homozygosity for A119S results in substantial levels of neural dysfunction (**Figure 3**). Despite these detrimental effects, we also find that A119S, even when heterozygous, confers a substantial survival advantage upon exposure to CGs. Such insights could only be provided by evaluating the effects of mutations in the context of the whole organism. Investigating just one aspect of phenotype, for example biochemistry *in vitro*, yielded a misleading picture of the fitness advantages, and disadvantages, that likely operate on the individual amino acid substitutions underlying this adaptation.

Our findings raise the question of how, given its deleterious effects, A119S became established in so many species. Initially, a survival advantage conferred by A119S in CG-rich environments may have outweighed deleterious effects associated with homozygosity for this substitution. This may be especially true for insects that specialized on CG-containing plants, where competition with other species for resources is reduced. In multiple lineages, the substitutions A119S and A119N preceded substitutions to 111 and 122 (Hemiptera, Hymenoptera, Diptera). In Drosophila, where we have the greatest phylogenetic resolution, A119S was established before substitutions to sites 111 and 122 in the evolutionary lineage leading to *D. subobscura*. This said, Q111L is sometimes observed in the absence of A119S (as is Q111E, see **Figure 1A**: *Bemisa tabaci* and *Lophocarya caryae;* not shown are *Aedes aegypti*, *Mechanitis polymia* and *Empyreuma pugione*, see **Figure S2**) implying alternative permissive substitutions in these taxa. More generally, A119S is not a particularly uncommon substitution among taxa that do not specialize on CG-containing hostplants (**Figure S2**), again implying the existence of additional compensatory substitutions in these species. None of the 18 sites distinguishing the *D. subobscura* and *D. melanogaster* proteins appear among sites most highly correlated with A119S in a phylogenetic analysis, however, leaving us few clues about promising candidates (**Figure S3**).

This said, a model invoking serial substitution of A119S and compensatory mutations is not the only plausible scenario. Alternatively, since CG-insensitive haplotypes substitutions including A119S lack strong deleterious effects and may confer a survival advantage upon

exposure to CGs when heterozygous (**Figure 3, Figure 4, Figure S8**), such haplotypes may be maintained over time by heterozygote advantage and subsequently reach fixation as they accumulate a sufficient number of compensatory substitutions (Kimura 1985) or by gene duplication (Spofford 1969), which has occurred repeatedly in CG-specialist species (Zhen et al. 2012; Petschenka et al. 2017; Yang et al. 2019). Interestingly, *D. subobscura* is polymorphic for substitutions at positons 111 and 122 mediating CG-insensitivity and these haplotypes are associated with polymorphic inversions that may rarely be homozygous (Pegueroles et al. 2016). The evolution of CG-insensitivity in *D. subobscura* may be recent and represent a transient stage in the evolution of this adaptive trait.

Our study adds to a growing body of work linking epistasis to the dynamics of adaptive evolution in contexts where the ecological relevance of the phenotype is well-understood (Tarvin et al. 2017; McGlothlin et al. 2016; Tufts et al. 2015; Kumar et al. 2017). To date, however, epistasis among substitutions in a protein has been evaluated *in silico*, *in vitro*, and in microbes along the dimensions of either protein folding stability, ligand specificity, enzyme activity, or cell growth rates (Storz 2016). While it is tempting to use one axis of the mutation-phenotype map as a convenient proxy for fitness (e.g. *in vitro* studies of the effects of mutations on protein function), the actual effect of a given mutation on fitness is a convolution over multiple phenotypes, from the levels of enzyme and tissue function to that of whole organism fitness in its environment. By considering phenotypic effects both *in vitro* and *in vivo*, we demonstrate how dominance and epistasis of amino acid substitutions can be missed or mischaracterized in the absence of a whole animal model to evaluate these effects. As such, our study reveals surprising new features of adaptive amino acid substitutions that were previously inaccessible.

Methods.

Sequencing and alignments.

Sources of data used in this study are detailed in **Table S1**. We collected new data for three species: *Drosophila subobscura* (Diptera), *Monophadnus latus* (Hymentoptera), and *Syntomeida epilais* (Lepidoptera). In each case, total RNA was extracted using TRIzol (Ambion, Life Technologies) following the manufacturer's protocol. RNA-seq libraries were prepared with either the TruSeq RNA Library Prep Kit v.2 (Illumina) or TruSeq Stranded RNA Library Prep Gold (Illumina) and sequenced on HiSeq2500 (Genomics Core Facility, Princeton, NJ, USA). 50-55 million paired-end 150 nucleotide reads per library were trimmed for quality (Phred quality ≥ 20) and length (≥30 contiguous bases). Trinity 2.2.0 (Haas et al. 2013) was used for *de novo* transcriptome assembly using default parameters. The ATPα1 coding sequences of *D. melanogaster* (FBgn0002921) and *B. mori* (GenBank: LC029030.1) were used to query the assembled transcripts using either tblastx or tblastn (blast-2.26). For *Dysdercus cingulatus* (Hemiptera), *Macrocheraia grandis* (Hemiptera), *Largus californicus* (Hemiptera), *Jalysus sp.* (Hemiptera), *Metatropis rufescens*, *Ischnodemus falicus*, *Geocoris sp.*, *Gyndes sp.*, *Monomorium pharaonis*, *Hylobius abietis*, *Megacyllene caryae*, *Calligrapha philadelphica*, and *Basilepta melanopus,* we downloaded raw RNA-seq data, carried out *de novo* assembly and obtained ATPα1 sequences using methods similar to those described above. The remaining ATPα1 sequences were either previously published or obtained from publicly available genome references assemblies. A multiple nucleotide sequence alignment was created using ClustalOmega (Sievers et al. 2011). Two alternatively spliced exons were masked for subsequent phylogenetic analyses.

Statistical phylogenetic analyses.

Phylogenetic relationships were established based on previously published sources (**Table S2**). Phylogeny branch lengths were estimated using IQtree (Nguyen et al. 2015) on the nucleotide alignment of 174 ATPα1 sequences representing 161 species sampled from 8 insect orders (**Figure S2**) using a guide phylogeny (**Figures S1**) to force species branching order within orders. We carried out a comprehensive search for substitutions at ATPα1 on which substitutions at sites 111 and 122 were dependent using BayesTraits (Pagel and Meade 2006). We first reconstructed the ancestral sequences of ATPα1 using PAML (Yang 2007). As inputs, we provided PAML with the phylogeny with branch lengths and the amino acid alignment for ATPα1. We used the default PAML parameters with the following changes:"cleandata" was set to 0 to preserve sites with missing data; "fix_blength" was set to 1 to use the branch lengths as the initial values in the ancestral reconstruction; "method" was set to 1 to use a new algorithm in PAML that updates branch lengths one-by-one. Using the inferred ancestor, we then binarized each amino acid state in the multi-species alignment into ancestral, "0", and derived, "1", and used this, and the phylogeny with branch lengths as the input for BayesTraits. BayesTraits fits a continuous-time Markov model to estimate transition rates between discrete, binary traits and calculates the likelihood of the fitted model. Restricting rate parameters appropriately (see below), we tested whether the transition rates for sites 111 and 122 were dependent on the state at all other variant sites. We excluded 56 sites with just a single substitution (i.e. one instance in 174 sequences in the alignment) due to their low information content.

In all models, double transition rates (e.g. Q111V and A119S occurring at the same time) were set to zero as double transitions are highly unlikely to occur in a single step and can be modeled as two single transitions, following Pagel (1994). Additionally, we set all transition rates from the derived state back to the ancestral state to zero as failing to do this resulted in unrealistically high estimates of the reversion rate. After these restrictions were imposed, the null model (i.e. independence) had four transition parameters. To test the dependence between sites, we refit an alternative model with two additional restrictions: one forcing the transition rate at site 1 to be fixed regardless of the state of site 2, and a second forcing the transition rate at site 2 to be fixed regardless of the state of site 1. This effectively tests whether the transition rate is affected by the state of either site.

Following the BayesTraits manual recommendations, the phylogeny branch lengths were scaled using BayesTraits to have a mean length of 0.1. Additionally, to increase the chance of finding the true maximum likelihood, we set MLTries to 250 which controls the number of times BayesTraits calls the maximum likelihood algorithm, returning the maximum likelihood of the 250 attempts. We ran each pair 25 times and checked that at least half of the runs had equivalent maximum likelihoods (within 0.1) to ensure that the results were stable. Taking the maximum likelihood for each pair, for each model, we calculated p-values using the LRT, where the statistic of merit is: 2 (unrestricted model – restricted model). The LRT statistic is distributed chi-squared with degrees of freedom (df) equal to the number of restrictions imposed on the model (df=2).

Engineering ATPα amino-acid substitution lines.

To test for phenotypic effects associated with candidate amino-acid substitutions, we developed a genetic engineering approach of the endogenous *ATPα1* (CG5670) locus in *Drosophila melanogaster*. Employing a strategy similar to that of Roland et al. (2013), we first generated a "founder line" by deletion of exons 2-6b and replacement with a functional *attP* element using ends-out homologous recombination (**Figure S10**). To generate the founder line, homology arms were generated as 2-3 kilobase PCR amplicons 5' of exon 2 and 3' of exon 6b and inserted into the *pGX-attP* vector (Huang et al. 2009). This construct was injected into w^{1118} embryos using standard protocols for P-element transgenesis (Rainbow Transgenic Flies, Inc.). Ends out recombination was performed and molecularly confirmed. The *mini-white* gene was subsequently removed by Cre-lox mediated excision (Groth et al. 2004) to create the founder line, w^{1118}*;;ATPαΔ2-6b attP/TM6B,Tb1* (exons 2-6b were replaced by a functional *attP* site).

To generate allelic variant lines of ATPα1, we cloned exons 2-6b into *pGX-attB-ATPα2-6b* vector and injected it into the *attP* founder line mated to *vasa-phiC31-ZH2A* flies using standard protocols (Rainbow Transgenic Flies, Inc). The unmodified plasmid was to generate a wild-type control (*GE-ATPα–Δ2-6b-WT*) following Cre-lox reduction of the *mini-white*. We then used site-directed mutagenesis (Quick-change Lightening, Agilent) to generate a panel of amino-acid substitution variants of *pGX-attB-ATPα2-6b* and corresponding GE strains were generated and Cre-lox reduced, as above for the WT control (**Table S3**). Variant and control lines were balanced by crossing to *w;;Dr[1]/TM6B, P{w[+mC]=Dfd-EYFP}3,* Sb^1*,*Tb^1*,*ca^1 (Bloomington Stock Center line 8704) and selecting for EYFP florescence. Homozygous variant GE-ATPα lines were established, when possible, by sib-mating and

selection of non-florescent *Tb*$^{+}$,*Sb*$^{+}$ larvae. All substitutions were confirmed using PCR and Sanger-based sequencing.

Viability assays.

Viability was measured in three ways. First, we measured viability as the relative hatchability of embryos carrying a given homozygous amino acid substitution (hereafter "Mut"). To do this, we self-crossed each balanced *GE-ATPα–Δ2-6b-Mut/TM6B, P{w[+mC]=Dfd-EYFP}3, Sb*^{1},*Tb*^{1},*ca*^{1} and allowed them to lay fertilized eggs on standard apple juice–agar Petri plates with yeast paste for two hours at 25°C, 50% humidity. After 24 hours, the relative proportion of non-EYFP (i.e. homozygous *Mut/Mut*) to EYFP (i.e. heterozygous *Mut*/+) first instar larvae were counted. As a control, we generated *GE-ATPα–Δ2-6b-WT/TM6B, P{w[+mC]=Dfd-EYFP}3, Sb*^{1},*Tb*^{1} *parents* and followed the same procedure. A second measure of viability is the probability of survival of a first instar *Mut/Mut* larvae to adulthood. To measure this, we transferred homozygous (*Mut/Mut*) first instar larvae to fly media vials (recipe R, LabExpress, Ann Arbor, MI). Larval density was limited to 10 per vial and vials were kept at 25°C, 50% humidity. After two weeks, we counted the number of emerging adults. Homozygous *GE-ATPα–Δ2-6b-WT* first instar larvae generated the same way were used as a control. Third, we measured egg-to-adult fitness as the proportion of emerging *Mut/Mut* adults in media bottles (recipe B, LabExpress, Ann Arbor, MI) seeded with *GE-ATPα–Δ2-6b-Mut/TM6B, P{w[+mC]=Dfd-EYFP}3, Sb*^{1},*Tb*^{1},*ca*^{1} parents and used bottles seeded with *+/TM6B, P{w[+mC]=Dfd-EYFP}3, Sb*^{1},*Tb*^{1},*ca*^{1} parents as controls.

Homozygous mutant (i.e. EYFP-) embryos represent ~1/4 of screened embryos. For series 1 engineered lines, Figure 1B, mean sample sizes for EYFP- individuals were 243 (range 153-344) for 1st instar larva | embryo, 62 (range 41-117) for pupa|larva, and 57 (range 31-117) for adult | larva. For series 2 engineered lines, Figure 1D, Mean sample sizes for EYFP- individuals were 203 (range 126-478) for 1st instar larva | embryo, 153 (range 99-344) for pupa|larva and adult | larva.

Enzyme inhibition assays.

For each *D. melanogaster* substitution line, we homogenized 90 heads (previously stored at -80°C) in 900 µl of deionized water, using a 1 ml glass grinder (Wheaton) chilled on ice (Petschenka et al. 2017). After vortexing, we divided homogenates into three aliquots of 300 µl representing technical replicates. Subsequently, samples were frozen at -80°C and freeze-dried (Christ, Alpha 2-4 LDPlus) overnight. For assessing resistance of NKA to ouabain, we followed the procedure as described in (Petschenka et al. 2013a) that is based on the photometric evaluation of phosphate released from enzymatic hydrolysis of adenosine triphosphate (ATP) as a measure of NKA activity. Lyophilisates were stored at -80°C until use and reconstituted with 500 µl deionized water. Head extractions were incubated at increasing concentrations of the water-soluble standard cardenolide ouabain (10^{-8} M to 2 x 10^{-3} M, Sigma, Germany, O3125-1G) at 37°C under the following conditions: 100 mM NaCl, 20 mM KCl, 4 mM $MgCl_2$, 50 mM imidazol, and 2.5 mM ATP (pH 7.4). We corrected all measurements for a background value that we obtained by incubating the extract under the same conditions as above, except with the addition of 2 x 10^{-3} M ouabain and no KCl (i.e., NKA inactive). On each microplate, we included an assay with porcine Na^+/K^+-ATPase (Sigma, Germany, A7510-5UN) as an internal

standard. In addition, we ran a series of KH_2PO_4 dilutions as a phosphate calibration curve on every plate. We measured absorbances at 700 nm using a CLARIOstar microplate reader (BMG Labtech, Germany). We carried out three biological replicates per line based on different extractions of fly heads. Each biological replicate was the average of three technical replicates, i.e. measurements based on aliquots from original extracts. For data analysis, we compared all measurements to a non-inhibited control. We fitted inhibition curves using OriginPro 2017 (OriginLab, Northampton, MA) with top and bottom asymptotes set to 100 and 0, respectively. Alternatively, we used least-squares fitting (using the nlsLM function of the minpack.lm library in R) to the bi-phasic curve function,

$$A = \mathrm{f}\left(1 - \frac{[I]}{[I]+IC_{50,1}}\right) + (1-f)\left(1 - \frac{[I]}{[I]+IC_{50,2}}\right),$$

where $IC_{50,1}$ and $IC_{50,2}$ represent the inhibitor concentration [I] required for 50% activity A of each isoform present in proportions f and $(1-f)$, respectively. Setting f=0 assumes a homogenous population of enzyme as expected for homozygotes. The two methods yielded similar IC_{50} estimates. Confidence intervals on estimates of $IC_{50,1}$, $IC_{50,2}$ and f were estimated using parametric bootstrap simulations, assuming that residuals across biological replicates are normally distributed.

Targeted allele-specific expression.

To estimate relative expression of mutant and wild-type alleles in heterozygous strains, we designed a targeted allele-specific expression (ASE) assay. Genomic DNA (gDNA) and total RNA were extracted sequentially using TRIzole Reagent (Invitrogen 15596026 and 15596018) from three replicate pools of 20 males sampled from each of sixteen lines. Extracted RNA was further purified with Qiagen RNAeasy column (Qiagen 74104) and reverse transcribed into cDNA with the use of random primers and ProtoScript II Reverse Transcriptase (NEB M0368S). Two sets of primers for ATPα1 were designed and used in subsequent PCR, multiplexing and sequencing. The first set were designed as exon-primed intron crossing (EPIC, Racle et al. 2017) primers and span a short intron separating exons 2 and 3. A second set of primers was used to add standard Illumina-like i5 and i7 barcodes to the PCR amplicons to facilitate multiplexing and subsequent sequencing. These multiplexed amplicons were pooled and sequenced on an Illimina MiSeq (Princeton Microarray Facility) and yielded ~1 million 150 nucleotide paired-end reads. Reads were mapped to gDNA and cDNA reference sequences using bwa-mem (Li 2013) and a Variant Calling File (VCF) file was produced using the Naive Variant Caller as implemented in Galaxy (Version 0.0.2). Allele counts at focal sites (104, 111 and 122) for both cDNA and gDNA were generated using a custom script. ASE was estimated using the Cochran-Mantel-Haenzel framework as implemented in R (mantelhaen.test). Specifically, ASE is estimated as the relative risk of the mutant substitution in the cDNA population using allele counts from gDNA as a reference population.

Behavioral phenotyping.

We quantified "bang sensitivity" which is a measure of susceptibility to seizures and paralysis upon mechanical over-stimulation (Ganetzky and Wu 1982). As such, the bang sensitivity phenotype is a measure of proper neuron function. Individual flies were placed in an empty fly media vial and vortexed at the maximum setting for 20 seconds. Immediately following mechanical overstimulation, neurologically dysfunctional flies typically experience a

period of convulsions and seizures. The recovery time was recorded as the time for each fly to right itself. Male flies were assayed 14 days post-eclosion. Approximate 95% confidence intervals were estimated around means by bootstrap resampling with replacement. An average of 43 flies were assayed (range 37-85). Recovery time distributions were compared using a Wilcoxon two-sample rank sum test with continuity correction as implemented in R (wilcox.test).

CG exposure assay.

As a measure of the ability to tolerate CGs, we exposed adult flies (1-7 days post-eclosion) to media containing known concentrations of the CG ouabain (Sigma). 1.5 grams of Drosophila instant media (Carolina Biological Supply) was reconstituted in a plastic vial with 7 mL of either 0, 5, 10 or 20 mM ouabain. After food solidified (30 min), a small paper wick was added. Three replicates of 10 males and 10 females were kept in each vial at 25°C and 50% humidity. Mortality was measured after 7 days. The genetically engineered wild-type line was used as a control. The Cochran-Mantel-Haenzel test framework (implemented in R) was used to assess significant differences between treatments (i.e. 5/10/20 mM ouabain versus no ouabain), as well as estimates and 95% confidence bounds for the relative risk associated with treatment. Odds Ratios (OR) estimated using this framework were converted into relative risk (RR) estimates using the formula, $RR = OR/(1 - p + (p * OR))$, where p is the risk in the no ouabain control group. A constant (0.5) was added to all cells to allow for calculation of relative risk in cases where mortality or survivors were absent. Thus, the maximum relative risk for this sample size (three replicates of 20 individuals each) is limited to 117. We found no sex differences in survival.

Acknowledgements:

We thank M. Przeworski and M. Schumer for comments on the manuscript, D. James and A. Wilson for sending *Syntomeida epilais* specimens and M. Aguadé for providing pre-publication access to the *D. guanche* ATPα1 sequence. We thank Sabrina Stiehler and Miyoung Yang for technical assistance. **Funding:** This work was funded by NIH R01 GM115523 to PA, NIH T32 GM008424 to BPR, NIH R01 GM108073 and NIH R01 AG027453 to MJP, and DFG PE 2059/3-1 and the LOEWE program of the State of Hesse (Insect Biotechnology & Bioresources), Germany to GP. **Author contributions:** PA, AMT, LY, and MJP designed the study; All authors contributed to the experimental work. PA wrote the paper. AMT, LY, AP, BPR, ADT, GP, and MJP reviewed and edited the manuscript.

Supplementary Materials

Figure S1. Cladogram showing relationships of sampled species.

Figure S2. Summary of amino acid variation at sites implicated in CG-sensitivity of ATPα1 in surveyed species.

Figure S3. Variant sites in ATPα1 most strongly correlated with substitutions with site 119.

Figure S4. Crystal structure of NKA bound to the cardiac glycoside ouabain (PDB:4HYT).

Figure S5. Enzyme inhibition curves for Q111V (V) with and without A119S (S).

Figure S6. Allele-specific expression (ASE) in heterozygous lines.

Figure S7. Bang sensitivity phenotypes of lines with heterozygous substitutions at sites 104, 111 and 122.

Figure S8. Bang sensitivity phenotypes of substitutions at sites 111 and 122 on the background of A119S.

Figure S9. Adult survival of homozygous strains with A119S upon 7-day exposure to CGs.

Figure S10. Engineering strategy for generating amino acid substitution lines.

Table S1. Sources of sequence data used in this study.

Table S2. References for phylogenetic relationships.

Table S3. Transgenic strains generated in this study.

References.

Ashmore LJ, Hrizo SL, Paul SM, Van Voorhies WA, Beitel GJ, Palladino MJ. 2009. Novel mutations affecting the Na, K ATPase alpha model complex neurological diseases and implicate the sodium pump in increased longevity. *Hum Genet* **126**: 431–447.

Bøttger P, Doğanlı C, Lykke-Hartmann K. 2012. Migraine- and dystonia-related disease-mutations of Na+/K+-ATPases: Relevance of behavioral studies in mice to disease symptoms and neurological manifestations in humans. *Neurosci Biobehav Rev* **36**: 855–871.

Brodie ED. 2009. Toxins and venoms. *Curr Biol* **19**: R931–R935.

Christin P-A, Salamin N, Savolainen V, Duvall MR, Besnard G. 2007. C4 Photosynthesis Evolved in Grasses via Parallel Adaptive Genetic Changes. *Curr Biol* **17**: 1241–1247.

Crambert G, Schaer D, Roy S, Geering K. 2004. New Molecular Determinants Controlling the Accessibility of Ouabain to Its Binding Site in Human Na,K-ATPase α Isoforms. *Mol Pharmacol* **65**: 335–341.

Dalla S, Dobler S. 2016. Gene duplications circumvent trade-offs in enzyme function: Insect adaptation to toxic host plants. *Evol Int J Org Evol* **70**: 2767–2777.

Dalla S, Swarts HGP, Koenderink JB, Dobler S. 2013. Amino acid substitutions of Na,K-ATPase conferring decreased sensitivity to cardenolides in insects compared to mammals. *Insect Biochem Mol Biol* **43**: 1109–1115.

Davis MW, Somerville D, Lee RY, Lockery S, Avery L, Fambrough DM. 1995. Mutations in the Caenorhabditis elegans Na,K-ATPase alpha-subunit gene, eat-6, disrupt excitable cell function. *J Neurosci* **15**: 8408–8418.

Dobler S, Dalla S, Wagschal V, Agrawal AA. 2012. Community-wide convergent evolution in insect adaptation to toxic cardenolides by substitutions in the Na,K-ATPase. *Proc Natl Acad Sci U S A* **109**: 13040–13045.

Dobler S, Petschenka G, Pankoke H. 2011. Coping with toxic plant compounds – The insect's perspective on iridoid glycosides and cardenolides. *Phytochemistry* **72**: 1593–1604.

Erb M, Robert CA. 2016. Sequestration of plant secondary metabolites by insect herbivores: molecular mechanisms and ecological consequences. *Curr Opin Insect Sci* **14**: 8–11.

Ganetzky B, Wu CF. 1982. Drosophila mutants with opposing effects on nerve excitability: genetic and spatial interactions in repetitive firing. *J Neurophysiol* **47**: 501–514.

Groen SC, LaPlante ER, Alexandre NM, Agrawal AA, Dobler S, Whiteman NK. 2017. Multidrug transporters and organic anion transporting polypeptides protect insects against the toxic effects of cardenolides. *Insect Biochem Mol Biol* **81**: 51–61.

Groth AC, Fish M, Nusse R, Calos MP. 2004. Construction of transgenic Drosophila by using the site-specific integrase from phage phiC31. *Genetics* **166**: 1775–1782.

Haas BJ, Papanicolaou A, Yassour M, Grabherr M, Blood PD, Bowden J, Couger MB, Eccles D, Li B, Lieber M, et al. 2013. De novo transcript sequence reconstruction from RNA-seq using the Trinity platform for reference generation and analysis. *Nat Protoc* **8**: 1494–1512.

Jerison ER, Desai MM. 2015. Genomic investigations of evolutionary dynamics and epistasis in microbial evolution experiments. *Curr Opin Genet Dev* **35**: 33–39.

Kimura M. 1985. The role of compensatory neutral mutations in molecular evolution. *J Genet* **64**: 7.

Kumar A, Natarajan C, Moriyama H, Witt CC, Weber RE, Fago A, Storz JF. 2017. Stability-Mediated Epistasis Restricts Accessible Mutational Pathways in the Functional Evolution of Avian Hemoglobin. *Mol Biol Evol* **34**: 1240–1251.

Li H. 2013. Aligning sequence reads, clone sequences and assembly contigs with BWA-MEM. *ArXiv13033997 Q-Bio*. http://arxiv.org/abs/1303.3997 (Accessed May 3, 2019).

Lingrel JB. 2010. The Physiological Significance of the Cardiotonic Steroid/Ouabain-Binding Site of the Na,K-ATPase. *Annu Rev Physiol* **72**: 395–412.

Liu Y, Cotton JA, Shen B, Han X, Rossiter SJ, Zhang S. 2010. Convergent sequence evolution between echolocating bats and dolphins. *Curr Biol CB* **20**: R53-54.

Losos JB. 2017. *Improbable Destinies: Fate, Chance, and the Future of Evolution*. First Edition edition. Riverhead Books, New York.

Matos-Cruz V, Schneider ER, Mastrotto M, Merriman DK, Bagriantsev SN, Gracheva EO. 2017. Molecular Prerequisites for Diminished Cold Sensitivity in Ground Squirrels and Hamsters. *Cell Rep* **21**: 3329–3337.

McGlothlin JW, Kobiela ME, Feldman CR, Castoe TA, Geffeney SL, Hanifin CT, Toledo G, Vonk FJ, Richardson MK, Brodie ED, et al. 2016. Historical Contingency in a Multigene Family Facilitates Adaptive Evolution of Toxin Resistance. *Curr Biol CB* **26**: 1616–1621.

Meyer WK, Jamison J, Richter R, Woods SE, Partha R, Kowalczyk A, Kronk C, Chikina M, Bonde RK, Crocker DE, et al. 2018. Ancient convergent losses of Paraoxonase 1 yield potential risks for modern marine mammals. *Science* **361**: 591–594.

Morris DH, Gostic KM, Pompei S, Bedford T, Łuksza M, Neher RA, Grenfell BT, Lässig M, McCauley JW. 2018. Predictive Modeling of Influenza Shows the Promise of Applied Evolutionary Biology. *Trends Microbiol* **26**: 102–118.

Nguyen L-T, Schmidt HA, von Haeseler A, Minh BQ. 2015. IQ-TREE: A Fast and Effective Stochastic Algorithm for Estimating Maximum-Likelihood Phylogenies. *Mol Biol Evol* **32**: 268–274.

Pagel M. 1994. Detecting correlated evolution on phylogenies: a general method for the comparative analysis of discrete characters. *Proc R Soc Lond B Biol Sci* **255**: 37–45.

Pagel M, Meade A. 2006. Bayesian Analysis of Correlated Evolution of Discrete Characters by Reversible-Jump Markov Chain Monte Carlo. *Am Nat* **167**: 808–825.

Palladino MJ, Bower JE, Kreber R, Ganetzky B. 2003. Neural Dysfunction and Neurodegeneration inDrosophila Na+/K+ ATPase Alpha Subunit Mutants. *J Neurosci* **23**: 1276–1286.

Pegueroles C, Ferrés-Coy A, Martí-Solano M, Aquadro CF, Pascual M, Mestres F. 2016. Inversions and adaptation to the plant toxin ouabain shape DNA sequence variation within and between chromosomal inversions of *Drosophila subobscura*. *Sci Rep* **6**: 23754.

Petschenka G, Fandrich S, Sander N, Wagschal V, Boppré M, Dobler S. 2013a. Stepwise evolution of resistance to toxic cardenolides via genetic substitutions in the Na+/K+ -ATPase of milkweed butterflies (lepidoptera: Danaini). *Evol Int J Org Evol* **67**: 2753–2761.

Petschenka G, Pick C, Wagschal V, Dobler S. 2013b. Functional evidence for physiological mechanisms to circumvent neurotoxicity of cardenolides in an adapted and a non-adapted hawk-moth species. *Proc R Soc B Biol Sci* **280**. https://www.ncbi.nlm.nih.gov/pmc/articles/PMC3619502/ (Accessed March 18, 2019).

Petschenka G, Wagschal V, von Tschirnhaus M, Donath A, Dobler S. 2017. Convergently Evolved Toxic Secondary Metabolites in Plants Drive the Parallel Molecular Evolution of Insect Resistance. *Am Nat* **190**: S29–S43.

Puerma E, Orengo DJ, Cruz F, Gómez-Garrido J, Librado P, Salguero D, Papaceit M, Gut M, Segarra C, Alioto TS, et al. 2018. The High-Quality Genome Sequence of the Oceanic Island Endemic Species Drosophila guanche Reveals Signals of Adaptive Evolution in Genes Related to Flight and Genome Stability. *Genome Biol Evol* **10**: 1956–1969.

Racle J, Jonge K de, Baumgaertner P, Speiser DE, Gfeller D. 2017. Simultaneous enumeration of cancer and immune cell types from bulk tumor gene expression data. *eLife*. https://elifesciences.org/articles/26476 (Accessed April 22, 2019).

Roland BP, Stuchul KA, Larsen SB, Amrich CG, Vandemark AP, Celotto AM, Palladino MJ. 2013. Evidence of a triosephosphate isomerase non-catalytic function crucial to behavior and longevity. *J Cell Sci* **126**: 3151–3158.

Schoner W. 2002. Endogenous cardiac glycosides, a new class of steroid hormones. *Eur J Biochem* **269**: 2440–2448.

Schubiger M, Feng Y, Fambrough DM, Palka J. 1994. A mutation of the drosophila sodium pump α subunit gene results in bang-sensitive paralysis. *Neuron* **12**: 373–381.

Sievers F, Wilm A, Dineen D, Gibson TJ, Karplus K, Li W, Lopez R, McWilliam H, Remmert M, Söding J, et al. 2011. Fast, scalable generation of high-quality protein multiple sequence alignments using Clustal Omega. *Mol Syst Biol* **7**: 539.

Spofford JB. 1969. Heterosis and the Evolution of Duplications. *Am Nat* **103**: 407–432.

Stern DL. 2011. *Evolution, Development and the Predictable Genome.* Roberts and Company Publishers, Greenwood Village, CO.

Stern DL. 2013. The genetic causes of convergent evolution. *Nat Rev Genet* **14**: 751–764.

Storz JF. 2016. Causes of molecular convergence and parallelism in protein evolution. *Nat Rev Genet* **17**: 239–250.

Storz JF. 2018. Compensatory mutations and epistasis for protein function. *Curr Opin Struct Biol* **50**: 18–25.

Tarvin RD, Borghese CM, Sachs W, Santos JC, Lu Y, O'Connell LA, Cannatella DC, Harris RA, Zakon HH. 2017. Interacting amino acid replacements allow poison frogs to evolve epibatidine resistance. *Science* **357**: 1261–1266.

Torrie LS, Radford JC, Southall TD, Kean L, Dinsmore AJ, Davies SA, Dow JAT. 2004. Resolution of the insect ouabain paradox. *Proc Natl Acad Sci U S A* **101**: 13689–13693.

Tufts DM, Natarajan C, Revsbech IG, Projecto-Garcia J, Hoffmann FG, Weber RE, Fago A, Moriyama H, Storz JF. 2015. Epistasis Constrains Mutational Pathways of Hemoglobin Adaptation in High-Altitude Pikas. *Mol Biol Evol* **32**: 287–298.

Vaughan GL, Jungreis AM. 1977. Insensitivity of lepidopteran tissues to ouabain: Physiological mechanisms for protection from cardiac glycosides. *J Insect Physiol* **23**: 585–589.

Yang. 2007. PAML 4: Phylogenetic Analysis by Maximum Likelihood. *Mol Biol Evol* **24**: 1586–1591.

Yang L, Ravikanthachari N, Marino-Perez R, Deshmukh R, Wu M, Rosenstein A, Kunte K, Song H, Andolfatto P. 2019. Predictability in the evolution of Orthopteran cardenolide insensitivity. *bioRxiv* 542811.

Zhen Y, Aardema ML, Medina EM, Schumer M, Andolfatto P. 2012. Parallel molecular evolution in an herbivore community. *Science* **337**: 1634–1637.

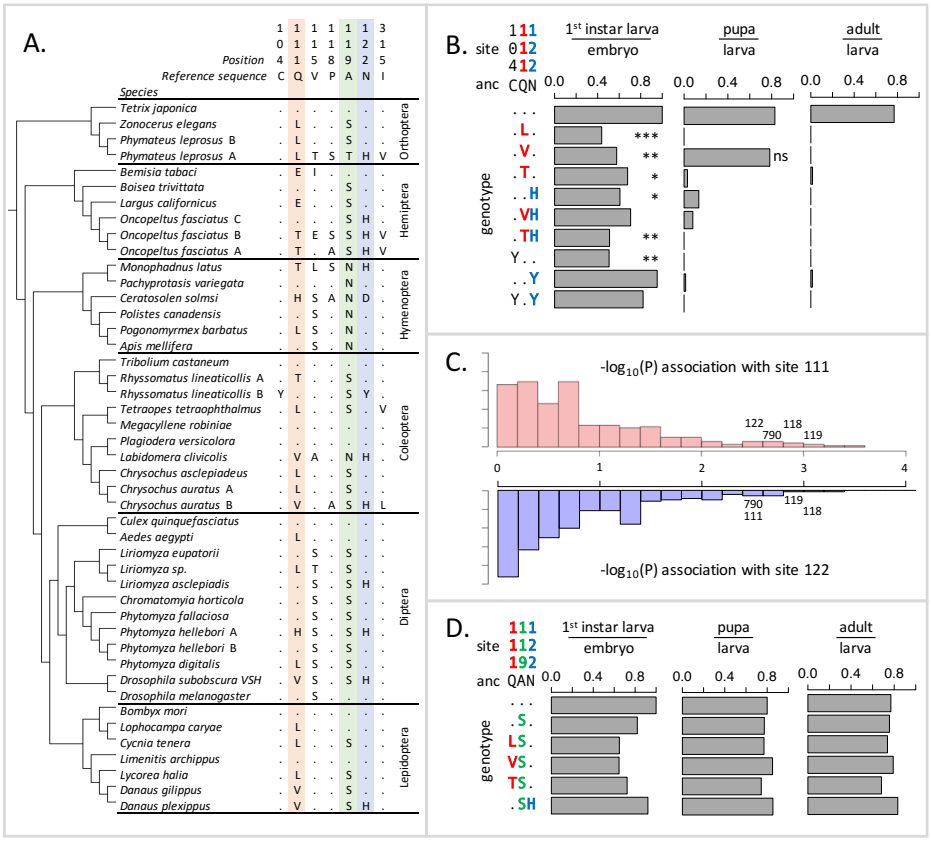

Figure 1. Deleterious effects of substitutions at positions 111 and 122 are ameliorated by the permissive substitution A119S. (**A)** Patterns of amino acid substitution at sites implicated in CG sensitivity near the H1-H2 transmembrane domain of ATPα1 in representative species from six insect orders (see **Figure S2** for all species). Dots indicate identity with the ancestral reference sequence and letters indicate derived amino acid substitutions. Positions 111 and 122, highlighted in pink and blue respectively, are hotspots of frequent parallel substitution. C104Y and N122Y represent rare substitutions associated with ATPα1 duplication (Zhen et al. 2012). Position 119 (highlighted in green) had not been previously implicated in CG sensitivity, but is identified as a candidate permissive substitution in subsequent analyses. (**B)** Viability of homozygous first instar larvae, pupae and adults for the first series of engineered substitution lines. Plotted is the proportion of surviving homozygous mutant offspring (i.e. EYFP-), scaled by the proportion for the wild-type control. Dots indicate identity with the ancestral reference at sites C104, Q111, and N122. Adjusted Fisher's Exact Test P-values versus the wild-type strain: *** P<0.001; ** P<0.01, *P<0.05. All larvae to pupa survivorship are significantly lower than wild-type (P<1e-5) except for Q111V. All larvae to adult survivorship are significantly lower than wild-type (P<1e-5). (**C)** Distributions of P-values for the strength of the phylogenetic correlation between sites 111 (above) or 122 (below) and 270 non-singleton amino acid variants in a multi-sequence alignment including 174 ATPα1 sequences representing 161 species. Sites 111 and 122 exhibit highly correlated evolution. Three additional sites in the lowest 5% of P-values shared in common between sites 111 and 122, including site 119, are labelled. (**D)** Viability of homozygous first instar larvae, pupae and adults for the second series of engineered substitution lines that include A119S relative to the wild-type control. Dots indicate identity with the ancestral reference at sites Q111, A119, and N122. Despite slight reductions in viability, all reductions are not significant relative to wild-type line after multiple test correction.

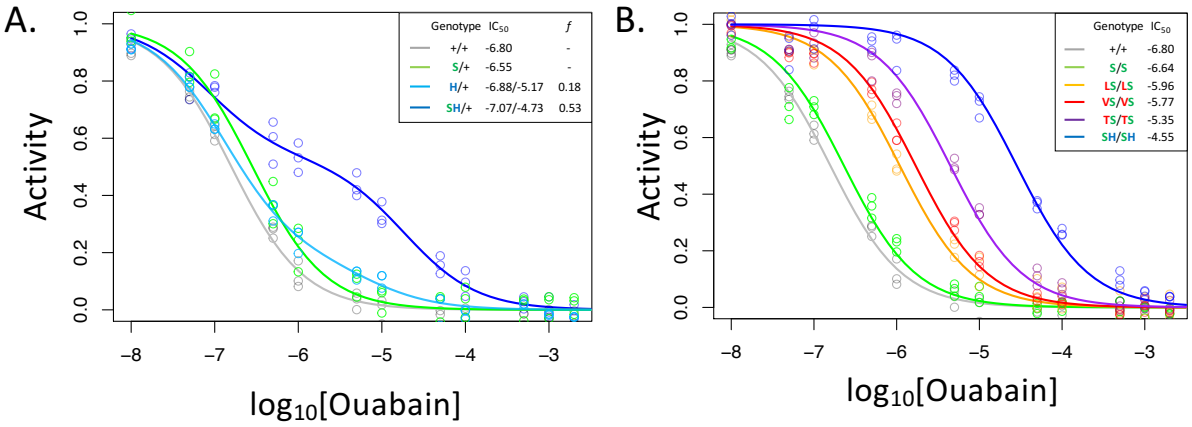

Figure 2. A119S ameliorates detrimental effects of CG-insensitivity substitutions on NKA function. Plotted are relative activity as a function of increasing concentrations of the cardiac glycoside (CG) ouabain. (A) Inhibition curves are plotted for heterozygous individuals to allow comparison of the effects of these substitutions in the presence and absence of A119S. Points represent biological replicates, each of which is the mean across three technical replicates. Curves for the engineered wild-type strain (+/+) and A119S/+ (S/+) are plotted for comparison. The presence of A119S alone confers a negligible increase in CG-insensitivity and results in a monophasic curve. In contrast, N122H/+ (H/+) and A119S+N122H (SH/+) exhibit a biphasic curves. The estimated proportion of CG-inhibitable activity of the mutant form for H/+, f = 0.18 (95% CI 0.14 - 0.24), is significantly lower than that of SH/+, f = 0.53 (95% CI 0.47 - 0.56). (B) Inhibition curves for homozygous substitutions Q111L, Q111V, Q111T and N122H in the presence of A119S reveal that they increase CG-insensitivity by 7, 11, 28 and 178-fold, respectively. The effect of A119S alone is estimated to be 1.45-fold relative to +/+ (95% CI 1.13 – 1.86).

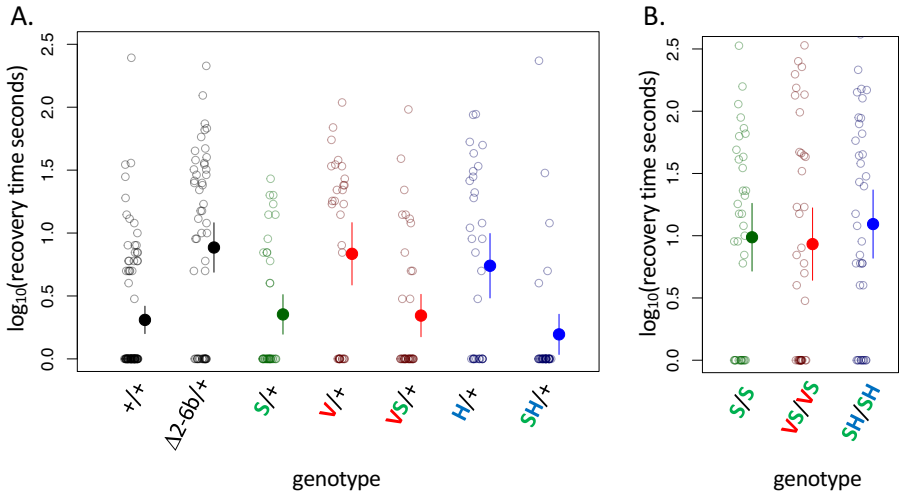

Figure 3. A119S ameliorates detrimental effects of CG-insensitivity substitutions on neural function. Plotted are recovery times for individuals (open circles), and means with approximate 95% confidence bounds (solid circles with whiskers), following mechanical over-stimulation (aka, the "bang sensitivity" assay). Flies heterozygous for loss-of-function ATPα1 substitutions are known to have significantly longer recovery times than wild-type flies (see for e.g. Δ2-6b/+ relative to +/+ in panel A, *P*=4.5e-7). **(A)** Distributions of recovery times for heterozygous flies (i.e. Mut/+) carrying individual substitutions A119S (S/+), Q111V (V/+) and N122H (H/+) and combinations VS/+ and SH/+. The recovery-time distributions for S/+, VS/+ and SH/+ are indistinguishable from the engineered wild-type strain (+/+). In contrast, recovery times are significantly longer than wild-type for lines with individual substitutions V/+ and H/+ (*P*=1.3e-5 and *P*=5.2e-4, respectively) and are indistinguishable from the loss-of-function deletion mutation Δ2-6b/+. (B) Recovery times for homozygous lines S/S, VS/VS and SH/SH are all significantly longer than for heterozygotes S/+, VS/+, and SH/+ (*P*<3.3e-3). These results demonstrate epistasis between substitutions at sites 119 and 111/122 at the level of neural function. A119 ameliorates the dominant dysfunction caused by Q111V and N122H but residual recessive neural dysfunction is still apparent in homozygotes that include A119S.

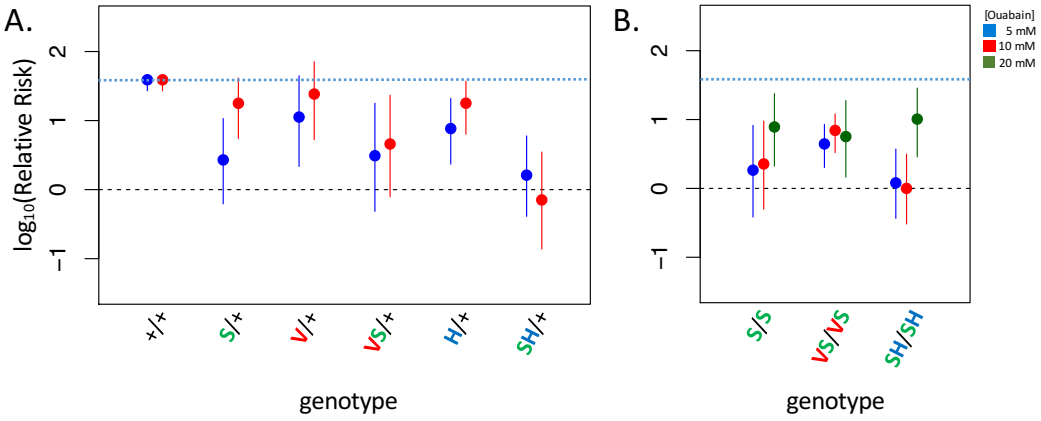

Figure 4. Adult survival upon 7-day exposure to the CG ouabain. Plotted is the log relative risk for treatments (5, 10 or 20 mM ouabain) relative to no treatment controls (no ouabain) for (A) heterozygous strains and (B) homozygous strains. Estimates (points) and 95% confidence bounds (whiskers) were obtained using the Cochran-Mantel-Haenzel framework. Each estimate is based on three biological replicates of 20 flies per concentration. A value of 0 corresponds to equal probability of survival on treatment versus the no ouabain control indicating complete insensitivity to a given concentration of ouabain. Labels: + = engineered wild-type allele; S = A119S; V = Q111V; VS = Q111V+A119S; H = N122H; SH = A119S+N122H. These results reveal appreciable CG-insensitivity conferred by individual substitutions A119S (S/+ and S/S) and the recessive lethals Q111V (V/+) and N122H (H/+) compared to the engineered wild-type control strain (+/+).

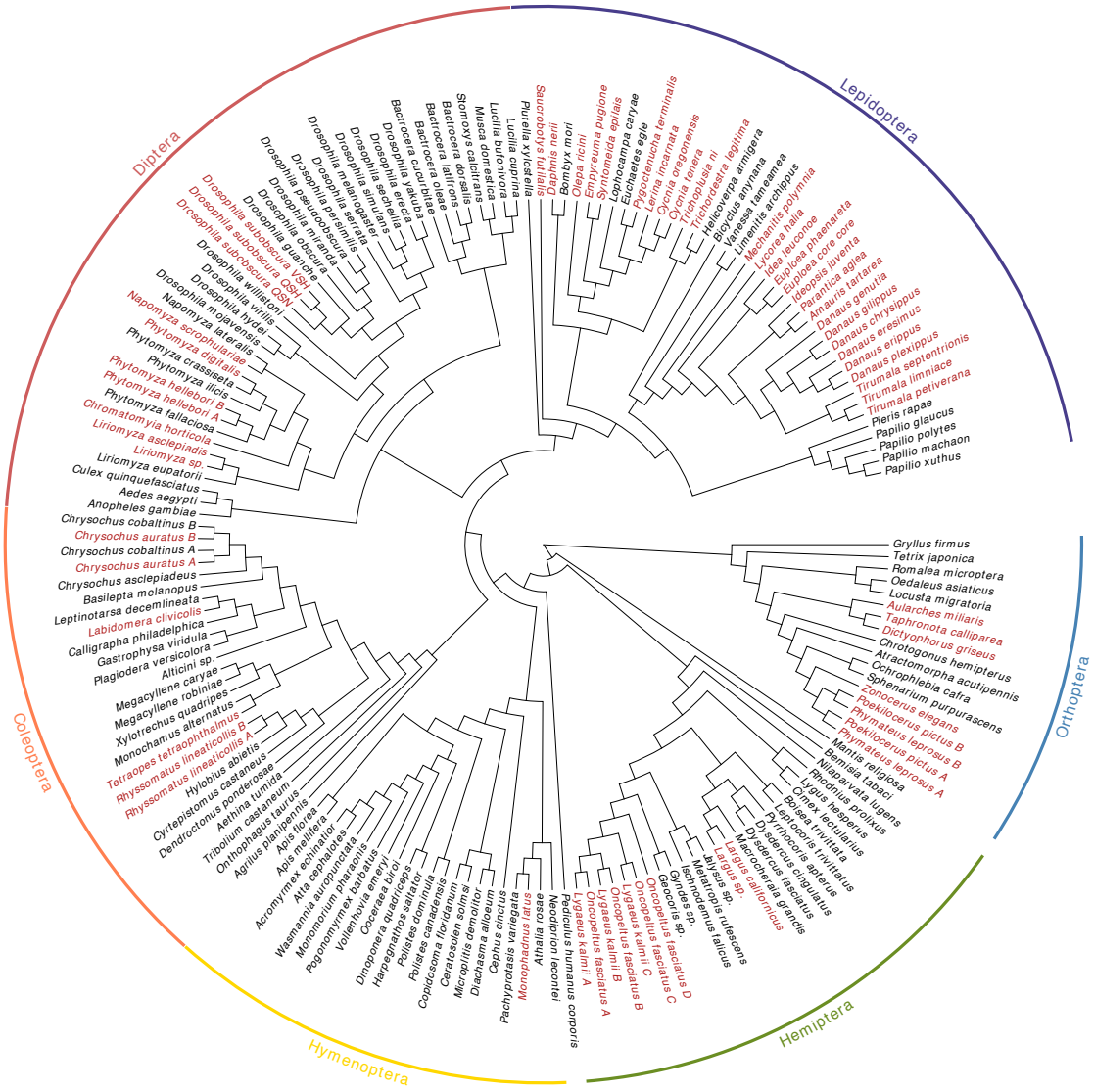

Supplementary Figure S1. Phylogeny showing relationships of sampled species. In red are species known specialists on CG-containing plants or inferred to be CG-insensitive.

Supplementary Figure S2. Summary of amino acid variation at sites implicated in cardenolide-sensitivity in ATPα1 in surveyed species

Position	100	108	111	112	114	115	116	117	118	119	122	123	124	128	129	132	133	134	135	136	139	140	141	142	143	144	145	146	147	148	149	150	151	152	153	154	155	156	157	158	159	160	161	162	specialists	outgroups
Reference sequence	C	Y	Q	A	T	V	E	E	P	A	D	D	N	Y	D	V	I	F	G	V	A	N	L	A	T	C	A	P	F	F	I	L	T	C	D	F	L	R	K	E	R	L		
Species																																														
Orthoptera																																													6	9
Gryllus firmus	.	.	.	.	.	.	.	.	D	.	S	.	.	.	.	.	.	.	.	.	.	.	.	.	.	.	.	.	.	.	.	.	.	.	.	.	.	.	.	.	.	.	.	.	.		
Tetrix japonica	.	.	.	.	.	.	.	.	.	.	.	.	.	.	.	.	.	.	.	.	.	.	.	.	.	.	.	.	.	.	.	.	.	.	.	.	.	.	.	.	.	.	.	.	.		
Romalea microptera	.	.	L	.	.	.	.	.	.	S	.	.	.	.	.	.	.	.	.	.	.	.	.	.	.	.	.	.	.	.	.	.	.	.	.	.	.	.	.	.	.	.	.	.	.		
Oedaleus asiaticus	.	.	L	.	.	.	.	.	.	S	.	.	.	.	.	.	.	.	.	.	.	.	.	.	.	.	.	.	.	.	.	.	.	.	.	.	.	.	.	.	.	.	.	.	.		
Locusta migratoria	.	.	L	.	.	.	.	.	.	S	.	.	.	.	.	.	.	.	.	.	.	.	.	.	.	.	.	.	.	.	.	.	.	.	.	.	.	.	.	.	.	.	.	.	.		
Aularches miliaris	.	.	L	.	.	.	.	.	.	S	.	.	.	.	.	.	.	.	.	.	.	.	.	.	.	.	.	.	.	.	.	.	.	.	.	.	.	.	.	.	.	.	.	.	.		
Taphronota calliparea	.	.	L	.	.	.	.	.	.	S	.	.	.	.	.	.	.	.	.	.	.	.	.	.	.	.	.	.	.	.	.	.	.	.	.	.	.	M	.	.	.	.	.	.	.		
Dictyophorus griseus	.	.	L	.	.	.	.	.	.	S	.	.	.	.	.	.	.	.	.	.	.	.	.	.	.	.	.	.	.	.	.	.	.	.	.	.	.	.	.	.	.	.	.	.	.		
Chrotogonus hemipterus	.	.	L	.	.	.	.	.	.	S	.	.	.	.	.	.	.	.	.	.	.	.	.	.	.	.	.	.	.	.	.	.	.	.	.	.	.	.	.	.	.	.	.	.	.		
Atractomorpha acutipennis	.	.	L	.	.	.	.	.	.	S	.	.	.	.	.	.	.	.	.	.	.	.	.	.	.	.	.	.	.	.	.	.	.	.	.	.	.	.	.	.	.	.	.	.	.		
Sphenarium purpurascens	.	.	L	.	.	.	.	.	.	S	.	.	.	.	.	.	.	.	.	.	.	.	.	.	.	.	.	.	.	.	.	.	.	.	.	.	.	M	.	.	.	.	.	.	.		
Ochrophlebia cafra	.	.	L	.	.	.	.	.	.	S	.	.	.	.	.	.	.	.	.	.	.	.	.	.	.	.	.	.	.	.	.	.	.	.	.	.	.	.	.	.	.	.	.	.	.		
Zonocerus elegans	.	.	L	.	.	.	.	.	.	S	.	.	.	.	.	.	.	.	.	.	.	.	.	.	.	.	.	.	.	.	.	.	.	.	.	.	.	.	.	.	.	.	.	.	.		
Poekilocerus pictus B	.	.	L	.	.	.	.	.	.	S	.	.	.	.	.	.	.	.	.	.	.	.	.	.	.	.	.	.	.	.	.	.	.	.	.	.	.	.	.	.	.	.	.	.	.		
Phymateus leprosus B	.	.	L	.	.	.	.	.	.	S	.	.	.	.	.	.	.	.	.	.	.	.	.	.	.	.	.	.	.	.	.	.	.	.	.	.	.	.	.	.	.	.	.	.	.		
Poekilocerus pictus A	.	.	L	.	.	T	.	.	S	S	.	.	H	.	.	V	.	.	.	.	.	.	.	.	.	.	.	.	.	.	M	.	.	.	.	.	.	.	.	.	.	.	.	.	.		
Phymateus leprosus A	.	.	L	.	.	T	.	.	S	T	E	N	H	.	.	V	.	.	.	.	.	.	.	.	.	.	.	.	.	.	M	.	.	.	.	.	.	M	.	.	.	.	.	.	.		
Mantodea																																													0	1
Mantis religiosa	.	.	.	.	.	.	.	.	.	.	.	.	.	.	.	.	.	.	.	.	.	.	.	.	.	.	.	.	.	.	.	.	.	.	.	.	.	.	.	.	.	.	.	.	.		
Hemiptera																																													4	16
Bemisia tabaci	.	.	E	S	.	I	.	.	.	.	.	.	.	.	E	.	.	.	.	.	.	.	.	.	.	.	.	.	.	.	V	.	V	.	.	.	M	.	.	.	.	.	.	.	.		
Nilaparvata lugens	.	.	.	.	.	.	.	.	.	.	.	.	.	.	.	.	.	.	.	.	.	.	.	.	.	.	.	.	.	.	.	.	.	.	.	.	M	.	.	.	.	.	.	.	.		
Rhodnius prolixus	.	.	.	.	.	.	.	.	.	S	.	.	.	.	.	.	.	.	.	.	.	.	.	.	.	.	.	.	.	.	.	.	.	.	.	.	M	.	.	.	.	.	.	.	.		
Lygus hesperus	.	.	.	.	.	.	.	.	.	.	.	.	.	.	.	.	.	.	.	.	.	.	.	.	.	.	.	.	.	.	.	.	.	.	.	.	T	.	.	.	.	.	.	.	.		
Cimex lectularius	.	.	.	.	.	.	.	.	.	S	.	.	.	.	.	.	.	.	.	.	.	.	.	.	.	.	.	.	.	.	.	.	.	.	.	.	M	.	.	.	.	.	.	.	.		
Boisea trivittata	.	.	.	.	.	.	.	.	.	S	.	.	.	.	.	.	.	.	.	.	.	.	.	.	.	.	.	.	.	.	.	.	.	.	.	.	T	.	.	.	.	.	.	.	.		
Leptocoris trivittatus	.	.	.	.	.	.	.	.	.	S	.	.	.	.	.	.	.	.	.	.	.	.	.	.	.	.	.	.	.	.	.	.	.	.	.	.	T	.	.	.	.	.	.	.	.		
Pyrrhocoris apterus	.	.	.	.	.	.	.	.	.	S	.	.	.	.	.	.	.	.	.	.	.	.	.	.	.	.	.	.	.	.	.	.	.	.	.	.	-	-	-	-	-	-	-	-	-		
Dysdercus cingulatus	.	.	.	.	.	.	.	.	.	S	.	.	.	.	.	.	.	.	.	.	.	.	.	.	.	.	.	.	.	.	.	.	.	.	.	.	M	.	.	.	.	.	.	.	.		
Dysdercus fasciatus	.	.	.	.	.	.	.	.	.	S	.	.	.	.	.	.	.	.	.	.	.	.	.	.	.	.	.	.	.	.	.	.	.	.	.	.	M	.	.	.	.	.	.	.	.		
Macrocheraia grandis	.	.	E	T	.	.	.	.	.	S	.	.	.	.	.	.	.	.	.	.	.	.	.	.	.	.	.	.	.	.	.	.	.	.	.	.	M	.	.	.	.	.	.	.	.		
Largus californicus	.	.	E	T	.	.	.	.	.	S	.	.	.	.	.	.	.	.	.	.	.	.	.	.	.	.	.	.	.	.	.	.	.	.	.	.	M	.	.	.	.	.	.	.	.		
Largus sp.	.	.	E	T	.	.	.	.	.	S	.	.	.	.	.	.	.	.	.	.	.	.	.	.	.	.	.	.	.	.	.	.	.	.	.	.	-	-	-	-	-	-	-	-	-		
Jalysus sp	.	.	.	.	.	.	.	.	.	S	.	.	.	.	.	.	.	.	.	.	.	.	.	.	.	.	.	.	.	.	.	.	.	.	.	.	K	.	.	.	.	.	.	.	.		
Metatropis rufescens	.	.	.	.	.	.	.	.	.	S	.	.	.	.	.	.	.	.	.	.	.	.	.	.	.	.	.	.	.	.	.	.	.	.	.	.	M	.	.	.	.	.	.	.	.		
Ischnodemus falicus	.	.	.	.	.	.	.	.	.	.	.	.	.	.	.	.	.	.	.	.	.	.	.	.	.	.	.	.	.	.	.	.	.	.	.	.	M	.	.	.	.	.	.	.	.		
Gyndes sp	.	.	.	.	.	.	.	.	.	S	.	.	.	.	.	.	.	.	.	.	.	.	.	.	.	.	.	.	.	.	.	.	.	.	.	.	M	.	.	.	.	.	.	.	.		
Geocoris sp	.	.	.	.	.	.	.	.	.	S	.	.	.	.	.	.	.	.	.	.	.	.	.	.	.	.	.	.	.	.	.	.	.	.	.	.	R	.	.	.	.	.	.	.	.		
Oncopeltus fasciatus D	.	.	.	.	.	.	.	.	.	S	.	.	H	.	.	.	.	.	.	.	.	.	.	.	.	.	.	.	.	.	.	.	.	.	.	.	V	.	.	.	.	.	.	.	.		
Oncopeltus fasciatus C	.	.	.	.	.	.	.	.	.	S	.	.	H	.	.	.	.	.	.	.	.	.	.	.	.	.	.	.	.	.	M	.	S	.	.	.	M	.	.	.	.	.	.	.	.		
Lygaeus kalmii C	.	.	.	.	.	.	.	.	.	S	.	.	H	.	.	.	.	.	.	.	.	.	.	.	.	.	.	.	.	.	M	.	S	.	.	.	M	.	.	.	.	.	.	.	.		
Oncopeltus fasciatus B	.	.	T	S	.	E	.	.	S	S	.	.	H	.	.	V	.	.	.	.	.	.	.	.	.	.	.	.	.	.	N	V	.	.	.	.	M	.	.	.	.	.	.	.	.		
Lygaeus kalmii B	.	.	T	S	.	E	.	.	S	S	.	.	H	.	.	V	.	.	.	.	.	.	.	.	.	.	.	.	.	.	N	V	.	.	.	.	M	.	.	.	.	.	.	.	.		
Oncopeltus fasciatus A	.	.	T	S	.	.	.	.	A	S	.	N	H	.	.	V	.	.	.	.	.	.	.	.	.	.	.	.	.	.	N	V	.	A	.	.	E	.	.	.	Q	.	.		
Lygaeus kalmii A	.	.	T	S	.	.	.	.	A	S	.	N	H	.	.	V	.	.	.	.	.	.	.	.	.	.	.	.	.	.	N	V	.	A	.	.	M	.	.	.	Q	.	.		
Phthiraptera																																												0	1
Pediculus humanus corporis	.	.	L	.	.	.	.	.	.	.	.	.	.	.	.	.	.	.	.	.	.	.	.	.	.	.	.	.	.	.	.	.	.	.	.	.	M	.	.	.	.	.	F				
Hymenoptera																																												1	21
Neodiprion lecontei	.	.	.	.	.	.	.	D	.	N	.	.	.	.	.	.	.	.	.	.	.	.	.	.	.	.	.	.	.	.	.	.	.	.	.	.	T	.	.	.	.	.	.	.	.		
Athalia rosae	.	.	.	.	.	.	.	D	.	N	.	.	.	.	.	.	.	.	.	.	.	.	.	.	.	.	.	.	.	.	.	.	.	.	.	.	.	.	.	.	.	.	.	.	.		
Monophadnus latus	.	.	T	.	.	L	.	.	S	N	.	.	H	.	.	.	.	.	.	.	.	.	.	.	.	.	.	.	.	.	M	.	.	.	.	.	T	.	.	.	.	.	.	.	.		
Pachyprotasis variegata	.	.	.	.	.	.	.	D	.	N	.	.	.	.	.	.	.	.	.	.	.	.	.	.	.	.	.	.	.	.	.	.	.	.	.	.	-	-	-	-	-	-	-	-	-		
Cephus cinctus	.	.	.	.	.	S	.	D	.	N	.	.	.	.	.	.	.	.	.	.	.	.	.	.	.	.	.	.	.	.	.	.	.	.	.	.	T	.	.	.	.	.	.	.	.		
Diachasma alloeum	.	.	.	.	.	S	.	D	.	N	.	.	.	.	.	.	.	.	.	.	.	.	.	.	.	.	.	.	.	.	.	.	.	.	.	.	T	.	.	.	.	.	.	.	.		
Microplitis demolitor	.	.	.	.	.	S	.	D	.	N	.	.	.	.	.	.	.	.	.	.	.	.	.	.	.	.	.	.	.	.	.	.	.	.	.	.	R	.	.	.	.	.	.	.	.		
Ceratosolen solmsi	.	.	H	.	.	S	.	D	A	N	E	.	D	.	.	.	.	.	.	.	.	.	.	.	.	.	.	.	.	.	.	.	.	.	.	.	T	.	.	.	.	.	.	.	.		
Copidosoma floridanum	.	.	.	.	.	S	D	.	.	N	.	.	.	.	.	.	.	.	.	.	.	.	.	.	.	.	.	.	.	.	.	.	.	.	.	.	R	.	.	.	.	.	.	.	.		
Polistes canadensis	.	.	.	.	.	S	.	D	.	N	.	.	.	.	.	.	.	.	.	.	.	.	.	.	.	.	.	.	.	.	.	.	.	.	.	.	.	.	.	.	.	.	.	.	.		
Polistes dominula	.	.	.	.	.	S	.	D	.	N	.	.	.	.	.	.	.	.	.	.	.	.	.	.	.	.	.	.	.	.	.	.	.	.	.	.	.	.	.	.	.	.	.	.	.		
Harpegnathos saltator	.	.	.	.	.	S	.	D	.	N	.	.	.	.	.	.	.	.	.	.	.	.	.	.	.	.	.	.	.	.	.	.	.	.	.	.	.	.	.	.	.	.	.	.	.		
Dinoponera quadriceps	.	.	.	.	.	S	.	D	.	N	.	.	.	.	.	.	.	.	.	.	.	.	.	.	.	.	.	.	.	.	.	.	.	.	.	.	.	.	.	.	.	.	.	.	.		
Ooceraea biroi	.	.	.	.	.	S	.	D	.	N	.	.	.	.	.	.	.	.	.	.	.	.	.	.	.	.	.	.	.	.	.	.	.	.	.	.	.	.	.	.	.	.	.	.	.		
Vollenhovia emeryi	.	.	.	.	.	S	.	D	.	N	.	.	.	.	.	.	.	.	.	.	.	.	.	.	.	.	.	.	.	.	.	.	.	.	.	.	.	.	.	.	.	.	.	.	.		
Pogonomyrmex barbatus	.	.	L	.	.	S	.	D	.	N	.	.	.	.	.	.	.	.	.	.	.	.	.	.	.	.	.	.	.	.	.	.	.	.	.	.	.	.	.	.	.	.	.	.	.		
Monomorium pharaonis	.	.	.	.	.	S	.	D	.	N	.	.	.	.	.	.	.	.	.	.	.	.	.	.	.	.	.	.	.	.	.	.	.	.	.	.	.	.	.	.	.	.	.	.	.		
Wasmannia auropunctata	.	.	.	.	.	S	.	D	.	N	.	.	.	.	.	.	.	.	.	.	.	.	.	.	.	.	.	.	.	.	.	.	.	.	.	.	M	.	.	.	.	.	.	.	.		
Atta cephalotes	.	.	.	.	.	S	.	D	.	N	.	.	.	.	.	.	.	.	.	.	.	.	.	.	.	.	.	.	.	.	.	.	.	.	.	.	.	.	.	.	.	.	.	.	.		

	1	1	1	1	1	1	1	1	1	1	1	1	1	3	3	3	3	3	3	3	3	3	3	3	3	3	6	7	7	7	7	7	8	8	8	8	8	8	9	9		
	0	0	1	1	1	1	1	1	1	1	2	2	2	0	1	1	1	1	2	2	2	3	3	3	3	5	6	7	8	8	8	9	9	0	0	6	7	8	8	9	7	8		
Position	4	8	1	2	4	5	6	7	8	9	0	1	2	8	2	4	5	6	9	2	3	4	0	1	8	7	6	8	3	6	7	3	7	2	4	3	4	0	6	8	2	2		
Reference sequence	C	Y	Q	A	T	V	E	E	P	A	D	D	N	Y	D	V	I	F	G	V	A	N	L	A	T	C	A	P	F	F	I	L	T	C	D	F	L	R	K	E	R	L		
Acromyrmex echinatior	.	.	.	.	.	S	.	D	.	N	.	.	.	.	.	.	.	.	.	.	.	.	.	.	.	.	.	.	.	.	.	.	.	.	.	.	.	.	.	.	.	.		
Apis mellifera	.	.	.	.	.	S	.	D	.	N	.	.	.	.	.	.	.	.	.	.	.	.	.	.	.	.	.	.	.	.	.	.	.	.	.	-	-	-	-	-	-	-		
Apis florea	.	.	.	.	.	S	.	D	.	N	.	.	.	.	.	.	.	.	.	.	.	.	.	.	.	.	.	.	.	.	.	.	.	.	.	.	.	.	.	.	.	.		
Coleoptera																																										5	18
Agrilus planipennis	.	.	.	.	.	.	.	.	.	.	.	.	.	.	.	.	.	.	.	.	.	.	.	.	.	.	.	.	.	.	.	.	.	.	.	.	A	.	.	.	.	.		
Onthophagus taurus	.	.	.	.	.	E	D	.	.	S	.	.	.	.	.	.	.	.	.	.	.	.	.	.	.	.	.	.	.	.	.	.	.	.	.	.	M	.	R	.	.	.		
Tribolium castaneum	.	.	.	.	.	.	.	.	.	.	.	.	.	.	.	.	.	.	.	.	.	.	.	.	.	.	.	.	.	.	.	.	.	.	.	.	T	.	.	.	.	.		
Aethina tumida	.	.	.	.	.	.	.	.	.	.	.	.	.	.	.	.	.	.	.	.	.	.	.	.	.	.	.	.	.	.	.	.	.	.	.	.	T	.	.	.	.	.		
Dendroctonus ponderosae	.	.	.	.	.	.	.	.	.	N	.	.	.	.	.	.	.	.	.	.	.	.	.	.	.	.	.	.	.	.	.	.	.	.	.	.	M	.	.	.	.	.		
Cyrtepistomus castaneus	.	.	.	.	.	.	.	.	.	.	.	.	.	.	.	.	.	.	.	.	.	.	.	.	.	.	.	.	.	.	.	.	.	.	.	.	M	.	.	.	.	.		
Hylobius abietis	.	.	L	.	.	.	.	.	.	.	.	.	.	.	.	.	.	.	.	.	.	.	.	.	.	.	.	.	.	.	.	.	.	.	.	.	M	.	.	.	.	.		
Rhyssomatus lineaticollis A	.	.	T	.	.	.	.	.	.	S	.	.	.	.	.	.	.	.	.	.	.	.	.	.	.	.	.	.	.	.	.	.	.	.	.	.	M	.	.	.	.	.		
Rhyssomatus lineaticollis B	Y	.	.	.	.	.	.	.	.	S	.	.	Y	.	.	.	.	.	.	.	.	.	.	.	.	.	.	.	.	.	.	.	.	.	.	.	M	.	.	.	.	.		
Tetraopes tetraophthalmus	.	.	L	.	.	.	.	.	.	S	.	.	.	.	.	.	V	.	.	.	.	.	.	.	.	.	.	.	.	.	.	.	.	.	.	.	R	.	.	.	.	.		
Monochamus alternatus	.	.	.	.	.	.	.	.	.	.	.	.	.	.	.	.	.	.	.	.	.	.	.	.	.	.	.	.	.	.	.	.	.	.	.	.	M	.	.	.	.	.		
Xylotrechus quadripes	.	.	.	.	.	.	.	.	.	.	.	.	.	.	.	.	.	.	.	.	.	.	.	.	.	.	.	.	.	.	.	.	.	.	.	.	R	.	.	.	.	.		
Megacyllene robiniae	.	.	.	.	.	.	.	.	.	.	.	.	.	.	.	.	.	.	.	.	.	.	.	.	.	.	.	.	.	.	.	.	.	.	.	.	R	.	.	.	.	.		
Megacyllene caryae	.	.	.	.	.	.	.	.	.	.	.	.	.	.	.	.	.	.	.	.	.	.	.	.	.	.	.	.	.	.	.	.	.	.	.	.	R	.	.	.	.	.		
Alticini sp.	.	.	.	.	.	.	.	.	.	.	.	.	.	.	.	.	.	.	.	.	.	.	.	.	.	.	.	.	.	.	.	.	.	.	.	-	-	-	-	-	-	-		
Plagiodera versicolora	.	.	.	.	.	.	.	.	.	.	.	.	.	.	.	.	.	.	.	.	.	.	.	.	.	.	.	.	.	.	.	.	.	.	.	.	M	.	.	.	.	.		
Gastrophysa viridula	.	.	.	.	.	.	.	.	.	.	.	.	.	.	.	.	.	.	.	.	.	.	.	.	.	.	.	.	.	.	.	.	.	.	.	.	M	.	.	.	-	-		
Calligrapha philadelphica	.	.	V	.	.	.	.	.	.	S	.	.	H	.	.	.	.	.	.	.	.	.	.	.	.	.	.	.	.	.	.	.	.	.	.	.	M	.	.	.	.	.		
Labidomera clivicolis	.	.	V	.	.	A	.	.	.	N	.	.	H	.	.	.	.	.	.	.	.	.	.	.	.	.	.	.	.	.	.	.	.	.	.	.	M	.	.	.	.	.		
Leptinotarsa decemlineata	.	.	V	.	.	.	.	.	.	N	.	.	.	.	.	.	.	.	.	.	.	.	.	.	.	.	.	.	.	.	.	.	.	.	.	.	M	.	.	.	.	.		
Basilepta melanopus	.	.	.	.	.	.	.	.	.	.	.	.	.	.	.	.	.	.	.	.	.	.	.	.	.	.	.	.	.	.	.	.	.	.	.	.	M	.	.	.	.	.		
Chrysochus asclepiadeus	.	.	L	.	.	.	.	.	.	S	.	.	.	.	.	.	.	.	.	.	.	.	.	.	.	.	.	.	.	.	M	.	.	.	.	-	-	-	-	-	-	-		
Chrysochus auratus A	.	.	L	.	.	.	.	.	.	S	.	.	.	.	.	.	.	.	.	.	.	.	.	.	.	.	.	.	.	.	.	.	.	.	.	.	M	.	.	.	.	.		
Chrysochus cobaltinus A	.	.	L	.	.	.	.	.	.	S	.	.	.	.	.	.	.	.	.	.	.	.	.	.	.	.	.	.	.	.	.	.	.	.	.	.	M	.	.	.	.	.		
Chrysochus auratus B	.	.	V	V	.	.	.	.	A	S	.	.	H	.	.	.	L	.	.	.	.	.	.	.	.	.	.	.	.	M	.	.	.	.	.	.	M	S	.	.	.	.		
Chrysochus cobaltinus B	.	.	V	V	.	.	.	.	A	S	.	.	H	.	.	.	L	.	.	.	.	.	.	.	.	.	.	.	.	M	.	.	.	.	.	.	M	.	.	.	.	.		
Diptera																																										7	31
Culex quinquefasciatus	.	.	.	.	.	.	.	.	.	.	.	.	.	.	.	.	.	.	.	.	.	.	.	.	.	.	.	.	.	.	.	.	.	.	.	.	.	.	.	.	.	.		
Aedes aegypti	.	.	L	.	.	.	.	.	.	.	.	.	.	.	.	.	.	.	.	.	.	.	.	.	.	.	.	.	.	.	.	.	.	.	.	.	.	.	.	.	.	.		
Anopheles gambiae	.	.	.	.	.	.	.	.	.	.	.	.	.	.	.	.	.	.	.	.	.	.	.	.	.	.	.	.	.	.	.	.	.	.	.	.	.	.	.	.	.	.		
Liriomyza eupatorii	.	.	.	.	.	S	.	.	.	S	.	.	.	.	.	.	.	.	.	.	.	.	.	.	.	.	.	.	.	.	.	.	.	.	.	-	-	-	-	-	-	-		
Liriomyza sp.	.	.	L	.	.	T	.	.	.	S	.	.	.	.	.	.	.	.	.	.	.	.	.	.	.	.	.	.	.	.	.	.	.	.	.	-	-	-	-	-	-	-		
Liriomyza asclepiadis	.	.	.	.	.	S	.	.	.	S	.	.	H	.	.	.	.	.	.	.	.	.	.	.	.	.	.	.	.	.	.	.	.	.	.	.	R	.	.	.	.	.		
Chromatomyia horticola	.	.	.	.	.	S	.	.	.	S	.	.	.	.	.	.	.	.	.	.	.	.	.	.	.	.	.	.	.	.	.	.	.	.	.	-	-	-	-	-	-	-		
Phytomyza fallaciosa	.	.	.	.	.	S	.	.	.	S	.	.	.	.	.	.	.	.	.	.	.	.	.	.	.	.	.	.	.	.	.	.	.	.	.	-	-	-	-	-	-	-		
Phytomyza hellebori A	.	.	H	.	.	S	.	.	.	S	.	.	H	.	.	.	.	.	.	.	.	.	.	.	.	.	.	.	.	M	.	.	.	.	.	-	-	-	-	-	-	-		
Phytomyza hellebori B	.	.	.	.	.	S	.	.	.	S	.	.	.	.	.	.	.	.	.	.	.	.	.	.	.	.	.	.	.	M	.	.	.	.	.	-	-	-	-	-	-	-		
Phytomyza ilicis	.	.	.	.	.	S	.	.	.	S	.	.	.	.	.	.	.	.	.	.	.	.	.	.	.	.	.	.	.	.	.	.	.	.	.	-	-	-	-	-	-	-		
Phytomyza crassiseta	.	.	.	.	.	S	.	.	.	S	.	.	.	.	.	.	.	.	.	.	.	.	.	.	.	.	.	.	.	.	.	.	.	.	.	-	-	-	-	-	-	-		
Phytomyza digitalis	.	.	L	.	.	S	.	.	.	S	.	.	.	.	.	.	.	.	.	.	.	.	.	.	.	.	.	.	.	.	.	.	.	.	.	-	-	-	-	-	-	-		
Napomyza scrophulariae	.	.	L	.	.	E	.	.	.	S	.	.	.	.	.	.	.	.	.	.	.	.	.	.	.	.	.	.	.	.	.	.	.	.	.	-	-	-	-	-	-	-		
Napomyza lateralis	.	.	L	.	.	E	.	.	.	S	.	.	.	.	.	.	.	.	.	.	.	.	.	.	.	.	.	.	.	.	.	.	.	.	.	-	-	-	-	-	-	-		
Drosophila mojavensis	.	.	.	.	.	S	.	.	.	S	.	.	.	.	.	.	.	.	.	.	.	.	.	.	.	.	.	.	.	.	.	.	.	.	.	.	M	.	.	.	.	F		
Drosophila hydei	.	.	.	.	.	S	.	.	.	S	.	.	.	.	.	.	.	.	.	.	.	.	.	.	.	.	.	.	.	.	.	.	.	.	.	.	M	.	.	.	.	F		
Drosophila virilis	.	.	.	.	.	S	.	.	.	S	.	.	.	.	.	.	.	.	.	.	.	.	.	.	.	.	.	.	.	.	.	.	.	.	.	.	M	.	.	.	.	F		
Drosophila willistoni	.	.	.	.	.	S	.	.	.	.	.	.	.	.	.	.	.	.	.	.	.	.	.	.	.	.	.	.	.	.	.	.	.	.	.	.	M	.	.	.	.	F		
Drosophila subobscura QSN	.	.	.	.	.	S	.	.	.	S	.	.	.	.	.	.	.	.	.	.	.	.	.	.	.	.	.	.	.	.	.	.	.	.	.	.	R	.	.	.	.	T		
Drosophila subobscura QSH	.	.	.	.	.	S	.	.	.	S	.	.	H	.	.	.	.	.	.	.	.	.	.	.	.	-	-	-	-	-	-	-	-	-	-	-	-	-	-	-	-	-		
Drosophila subobscura VSH	.	.	V	.	.	S	.	.	.	S	.	.	H	.	.	.	.	.	.	.	.	.	.	.	.	-	-	-	-	-	-	-	-	-	-	-	-	-	-	-	-	-		
Drosophila guanche	.	.	.	.	.	S	.	.	.	S	.	.	.	.	.	.	.	.	.	.	.	.	.	.	.	.	.	.	.	.	.	.	.	.	.	.	R	.	.	.	.	F		
Drosophila obscura	.	.	.	.	.	S	.	.	.	.	.	.	.	.	.	.	.	.	.	.	.	.	.	.	.	.	.	.	.	.	.	.	.	.	.	.	K	.	.	.	.	F		
Drosophila miranda	.	.	.	.	.	S	.	.	.	.	.	.	.	.	.	.	.	.	.	.	.	.	.	.	.	.	.	.	.	.	.	.	.	.	.	.	R	.	.	.	.	F		
Drosophila pseudoobscura	.	.	.	.	.	S	.	.	.	.	.	.	.	.	.	.	.	.	.	.	.	.	.	.	.	.	.	.	.	.	.	.	.	.	.	.	R	.	.	.	.	F		
Drosophila persimilis	.	.	.	.	.	S	.	.	.	.	.	.	.	.	.	.	.	.	.	.	.	.	.	.	.	.	.	.	.	.	.	.	.	.	.	.	R	.	.	.	.	F		
Drosophila serrata	.	.	.	.	.	S	.	.	.	.	.	.	.	.	.	.	.	.	.	.	.	.	.	.	.	.	.	.	.	.	.	.	.	.	.	.	K	.	.	.	.	F		
Drosophila melanogaster	.	.	.	.	.	S	.	.	.	.	.	.	.	.	.	.	.	.	.	.	.	.	.	.	.	.	.	.	.	.	.	.	.	.	.	.	K	.	.	.	.	F		
Drosophila simulans	.	.	.	.	.	S	.	.	.	.	.	.	.	.	.	.	.	.	.	.	.	.	.	.	.	.	.	.	.	.	.	.	.	.	.	.	K	.	.	.	.	F		
Drosophila sechellia	.	.	.	.	.	S	.	.	.	.	.	.	.	.	.	.	.	.	.	.	.	.	.	.	.	.	.	.	.	.	.	.	.	.	.	.	K	.	.	.	.	F		
Drosophila erecta	.	.	.	.	.	S	.	.	.	.	.	.	.	.	.	.	.	.	.	.	.	.	.	.	.	.	.	.	.	.	.	.	.	.	.	.	K	.	.	.	.	F		
Drosophila yakuba	.	.	.	.	.	S	.	.	.	.	.	.	.	.	.	.	.	.	.	.	.	.	.	.	.	.	.	.	.	.	.	.	.	.	.	.	K	.	.	.	.	F		
Bactrocera cucurbitae	.	.	.	.	.	S	.	.	.	S	.	.	.	.	.	.	.	.	.	.	.	.	.	.	.	.	.	.	.	.	.	.	.	.	.	.	M	.	.	.	.	.		
Bactrocera oleae	.	.	L	.	.	S	.	.	.	S	.	.	.	.	.	.	.	.	.	.	.	.	.	.	.	.	.	.	.	.	.	.	.	.	.	.	M	.	.	.	.	.		
Bactrocera latifrons	.	.	L	.	.	S	.	.	.	S	.	.	.	.	.	.	.	.	.	.	.	.	.	.	.	.	.	.	.	.	.	.	.	.	.	.	M	.	.	.	.	.		
Bactrocera dorsalis	.	.	L	.	.	S	.	.	.	S	.	.	.	.	.	.	.	.	.	.	.	.	.	.	.	.	.	.	.	.	.	.	.	.	.	.	M	.	.	.	.	.		
Stomoxys calcitrans	.	.	.	.	.	S	.	.	.	S	.	.	.	.	.	.	.	.	.	.	.	.	.	.	.	.	.	.	.	.	.	.	.	.	.	.	.	.	.	.	.	F		
Musca domestica	.	.	.	.	.	S	.	.	.	S	.	.	.	.	.	.	.	.	.	.	.	.	.	.	.	.	.	.	.	.	.	.	.	.	.	.	.	.	.	.	.	F		
Lucilia bufonivora	.	.	.	.	.	S	.	.	.	S	.	.	.	.	.	.	.	.	.	.	.	.	.	.	.	.	.	.	.	.	.	.	.	.	.	-	-	-	-	-	-	-		

	1	1	1	1	1	1	1	1	1	1	1	1	1	1	3	3	3	3	3	3	3	3	3	3	3	3	6	7	7	7	7	7	7	8	8	8	8	8	8	9	9
	0	0	1	1	1	1	1	1	1	1	1	2	2	2	0	1	1	1	1	2	2	2	3	3	3	6	5	7	8	8	8	9	9	0	0	6	7	8	8	9	7	8
Position	4	8	1	2	4	5	6	7	8	9	0	1	2	8	2	4	5	6	9	2	3	4	0	1	8	7	6	8	3	6	7	3	7	2	4	3	4	0	6	8	2	2
Reference sequence	C	Y	Q	A	T	V	E	E	P	A	D	D	N	Y	D	V	I	F	G	V	A	N	L	A	T	C	A	P	F	F	I	L	T	C	D	F	L	R	K	E	R	L
Lucilia cuprina	.	.	.	.	.	S	.	.	.	S	.	.	.	.	.	.	.	.	.	.	.	.	.	.	.	.	.	.	.	.	.	.	.	.	.	.	.	.	.	.	.	F
Lepidoptera																																									
Plutella xylostella	.	.	.	.	.	.	.	.	.	.	.	.	.	.	.	.	.	.	.	.	.	.	.	.	.	.	.	.	.	.	.	.	.	.	.	T	.	.	.	.	.	.
Saucrobotys futilalis	.	.	L	.	.	.	.	.	.	S	.	.	.	.	.	.	.	.	.	.	.	.	.	.	.	.	.	.	.	.	.	.	.	X	-	-	-	-	-	-	-	-
Daphnis nerii	.	.	L	.	.	.	.	.	.	S	.	.	.	.	.	.	.	.	.	.	.	.	.	.	.	.	.	.	.	.	.	.	.	.	.	M	.	.	.	.	.	.
Bombyx mori	.	.	.	.	.	.	.	.	.	.	.	.	.	.	.	.	.	.	.	.	.	.	.	.	.	.	.	.	.	.	.	.	.	.	.	M	.	.	.	.	.	.
Empyreuma pugione	.	.	L	.	.	.	.	.	.	.	.	.	.	.	.	.	.	.	.	.	.	.	.	.	.	.	.	.	.	.	.	.	.	.	-	-	-	-	-	-	-	-
Olepa ricini	.	.	.	.	.	.	.	.	.	.	.	.	.	.	.	.	.	.	.	.	.	.	.	.	.	.	.	.	.	.	.	.	.	.	.	.	.	.	.	.	.	.
Lerina incarnata	.	.	L	.	.	.	.	.	.	S	.	.	.	.	.	.	L	.	.	.	.	.	.	.	.	.	.	.	.	.	.	.	.	-	-	-	-	-	-	-	-	-
Pygoctenucha terminalis	.	.	L	.	.	.	.	.	.	S	.	.	.	.	.	.	.	.	.	.	.	.	.	.	.	.	.	.	.	.	.	.	.	.	-	-	-	-	-	-	-	-
Syntomeida epilais	.	.	L	.	.	E	.	.	.	S	.	.	.	.	.	.	.	.	.	.	.	.	.	.	.	.	.	.	.	.	.	.	.	.	.	.	.	.	.	.	.	.
Lophocampa caryae	.	.	L	.	.	.	.	.	.	.	.	.	.	.	.	.	.	.	.	.	.	.	.	.	.	.	.	.	.	.	.	.	.	.	.	.	.	.	.	.	.	.
Euchaetes egle	.	.	.	.	.	.	.	.	.	.	.	.	.	.	.	.	.	.	.	.	.	.	.	.	.	.	.	.	.	.	.	.	.	.	.	T	.	.	.	.	.	.
Cycnia oregonensis	.	.	.	.	.	.	.	.	.	.	.	.	.	.	.	.	.	.	.	.	.	.	.	.	.	.	.	.	.	.	.	.	.	.	-	-	-	-	-	-	-	-
Cycnia tenera	.	.	L	.	.	.	.	.	.	S	.	.	.	.	.	.	.	.	.	.	.	.	.	.	.	.	.	.	.	.	.	.	.	.	.	M	.	.	.	.	.	.
Trichoplusia ni	.	.	.	.	.	.	.	.	.	.	.	.	.	.	.	.	.	.	.	.	.	.	.	.	.	.	.	.	.	.	.	.	.	.	.	M	.	.	.	.	.	.
Trichordestra legitima	.	.	.	.	.	.	.	.	.	.	.	.	.	.	.	.	.	.	.	.	.	.	.	.	.	.	.	.	.	.	.	.	.	.	.	M	.	.	.	.	.	.
Helicoverpa armigera	.	.	.	.	.	.	.	.	.	.	.	.	.	.	.	.	.	.	.	.	.	.	.	.	.	.	.	.	.	.	.	.	.	.	.	M	.	.	.	.	.	.
Bicyclus anynana	.	.	.	.	.	.	.	.	.	.	.	.	.	.	.	.	.	.	.	.	.	.	.	.	.	.	.	.	.	.	.	.	.	.	.	.	.	.	.	.	.	.
Vanessa tameamea	.	.	.	.	.	.	.	.	.	S	.	.	.	.	.	.	.	.	.	.	.	.	.	.	.	.	.	.	.	.	.	.	.	.	.	.	.	.	.	.	.	.
Limenitis archippus	.	.	.	.	.	.	.	.	.	.	.	.	.	.	.	.	.	.	.	.	.	.	.	.	.	.	.	.	.	.	.	.	.	.	.	.	.	.	.	.	.	.
Mechanitis polymnia	.	.	L	.	.	.	.	.	.	.	.	.	.	.	.	.	.	.	.	.	.	.	.	.	.	.	.	.	.	.	.	.	.	.	.	T	.	-	-	-	-	-
Lycorea halia	.	.	L	.	.	.	.	.	.	S	.	.	.	.	.	.	.	.	.	.	.	.	.	.	.	.	.	.	.	.	.	.	.	.	.	T	.	.	.	.	.	.
Idea leuconoe	.	.	L	.	.	.	.	.	.	S	.	.	.	.	.	.	.	.	.	.	.	.	.	.	.	.	.	.	.	.	.	.	.	.	.	M	.	-	-	-	-	-
Euploea phaenareta	.	.	L	.	.	.	.	.	.	S	.	.	.	.	.	.	.	.	.	.	.	.	.	.	.	.	.	.	.	.	.	.	.	.	.	.	.	-	-	-	-	-
Euploea core core	.	.	L	.	.	.	.	.	.	S	.	.	.	.	.	.	.	.	.	.	.	.	.	.	.	.	.	.	.	.	.	.	.	.	.	M	.	.	.	.	.	.
Ideopsis juventa	.	.	L	.	.	.	.	.	.	S	.	.	.	.	.	.	.	.	.	.	.	.	.	.	.	.	.	.	.	.	.	.	.	.	.	-	-	-	-	-	-	-
Parantica aglea	.	.	L	.	.	.	.	.	.	S	.	.	.	.	.	.	.	.	.	.	.	.	.	.	.	.	.	.	.	.	.	.	.	.	.	-	-	-	-	-	-	-
Amauris tartarea	.	.	L	.	.	.	.	.	.	S	.	.	.	.	.	.	.	.	.	.	.	.	.	.	.	.	.	.	.	.	.	.	.	.	.	-	-	-	-	-	-	-
Danaus genutia	.	.	V	.	.	.	.	.	.	S	.	.	.	.	.	.	.	.	.	.	.	.	.	.	.	.	.	.	.	.	.	.	.	.	.	T	.	-	-	-	-	-
Danaus gilippus	.	.	V	.	.	.	.	.	.	S	.	.	.	.	.	.	.	.	.	.	.	.	.	.	.	.	.	.	.	.	.	.	.	.	.	T	.	.	.	.	.	.
Danaus chrysippus	.	.	V	.	.	.	.	.	.	S	.	.	.	.	.	.	.	.	.	.	.	.	.	.	.	.	.	.	.	.	.	.	.	.	.	T	.	.	.	.	.	.
Danaus eresimus	.	.	V	.	.	.	.	.	.	S	.	.	H	.	.	.	.	.	.	.	.	.	.	.	.	.	.	.	.	.	.	.	.	.	.	T	.	.	.	.	.	.
Danaus erippus	.	.	V	.	.	.	.	.	.	S	.	.	H	.	.	.	.	.	.	.	.	.	.	.	.	.	.	.	.	.	.	.	.	.	.	-	-	-	-	-	-	-
Danaus plexippus	.	.	V	.	.	.	.	.	.	S	.	.	H	.	.	.	.	.	.	.	.	.	.	.	.	.	.	.	.	.	.	.	.	.	.	T	.	.	.	.	.	.
Tirumala septentrionis	.	.	V	.	.	.	.	.	.	S	.	.	.	.	.	.	.	.	.	.	.	.	.	.	.	.	.	.	.	.	.	.	.	.	.	V	.	-	-	-	-	-
Tirumala limniace	.	.	V	.	.	.	.	.	.	S	.	.	.	.	.	.	.	.	.	.	.	.	.	.	.	.	.	.	.	.	.	.	.	.	.	V	.	-	-	-	-	-
Tirumala petiverana	.	.	V	.	.	.	.	.	.	S	.	.	.	.	.	.	.	.	.	.	.	.	.	.	.	.	.	.	.	.	.	.	.	.	.	V	.	-	-	-	-	-
Pieris rapae	.	.	.	.	.	.	.	.	.	.	.	.	.	.	.	.	.	.	.	.	.	.	.	.	.	.	.	.	.	.	.	.	.	.	.	.	.	.	.	.	.	.
Papilio glaucus	.	.	.	.	.	.	.	.	.	.	.	.	.	.	.	.	.	.	.	.	.	.	.	.	.	.	.	.	.	.	.	.	.	.	.	.	.	.	.	.	.	.
Papilio polytes	.	.	.	.	.	.	.	.	.	.	.	.	.	.	.	.	.	.	.	.	.	.	.	.	.	.	.	.	.	.	.	.	.	.	.	.	.	.	.	.	.	.
Papilio machaon	.	.	.	.	.	.	.	.	.	.	.	.	.	.	.	.	.	.	.	.	.	.	.	.	.	.	.	.	.	.	.	.	.	.	.	.	.	.	.	.	.	.
Papilio xuthus	.	.	.	.	.	.	.	.	.	.	.	.	.	.	.	.	.	.	.	.	.	.	.	.	.	.	.	.	.	.	.	.	.	.	.	.	.	.	.	.	.	.

NOTE - Columns correspond to 35 sites implicated in cardenolide-sensitivity with the addition of six additional sites of interest (112, 114, 119, 787, 874, 898). Following convention, position is standardized relative to the sheep (Ovis aries) sequence NM_001009360 - 5 AA from 5'end. The reference sequence refers to the consensus sequence among non-specialist species. A dot indicates identity with the reference sequence and dashes indicate missing data. Species highlighted in green are specialists on cardiac glycoside (CG) containing plants.

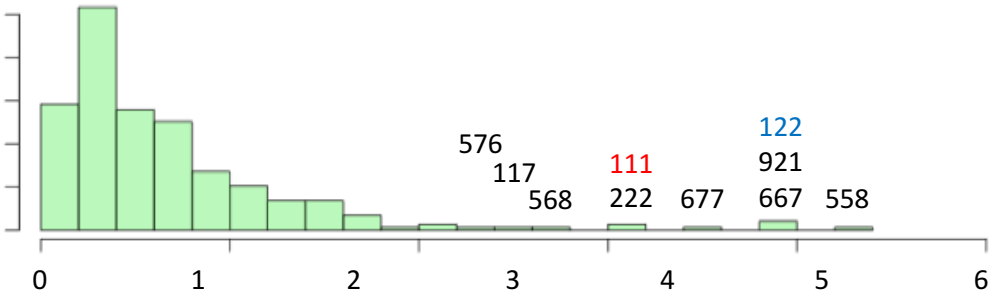

Supplementary Figure S3. Variant sites in ATPα1 most strongly correlated with substitutions with site 119. Shown is the distribution of P-values for strength of phylogenetic correlation between site 119 and 270 non-singleton amino acid variants in an alignment including 174 ATPα1 sequences representing 161 species See Methods for a description of estimating correlations using BayesTraits. Indicated are the 10 top ranking sites. Sites 111 (red) and 122 (blue) are highly-correlated interacting sites known to be important for insensitivity of the Na^+,K^+-ATPase to CG-inhibition (see Figure 1).

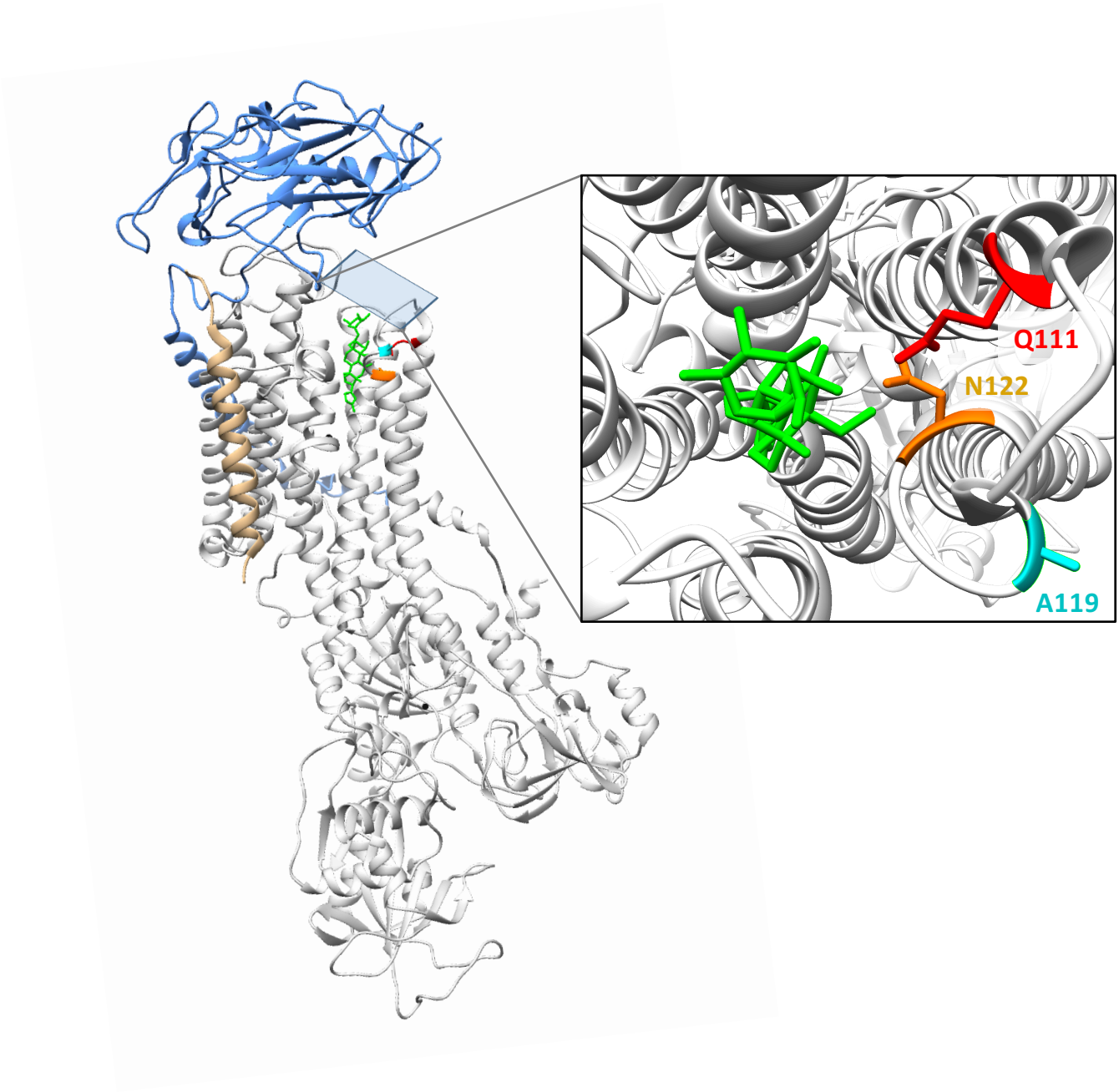

Supplementary Figure S4. Estimated co-crystal structure of *Drosophila melanogaster* Na^+,K^+-ATPase bound to the cardiac glycoside (CG) ouabain. A homology model was constructed with Swiss-Model (Waterhouse et al. 2018; https://swissmodel.expasy.org), using the *Sus scrofa* (pig) structure bound to ouabain (PDB:4HYT) as a template and ATPα1 of *D. melanogaster* (Genbank: P13607) as target. The alpha-subunit is shown in white ribbon, and subunits beta and gamma in blue and gold ribbon, respectively. In red, magenta and orange are residues Q111, A119 and N122, respectively. The bound ouabain ligand is colored green. The structure was visualized using UCSF Chimera 1.11.2.

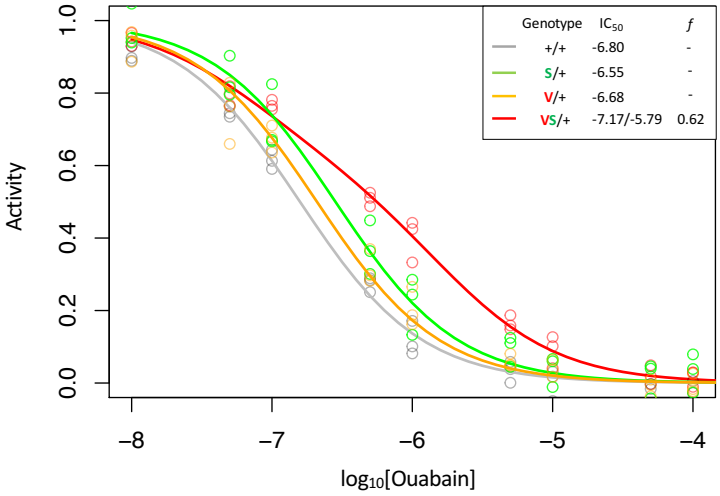

Supplementary Figure S5. Enzyme inhibition curves for Q111V (V) with and without A119S (S). Following Figure 2, inhibition curves are plotted for heterozygous individuals to allow comparison of the effects of these substitutions in the presence and absence of A119S. Points represent biological replicates, which is the means across technical replicates. Curves for the engineered wild-type strain (+/+) and A119S/+ are plotted for comparison. The presence of A119S or Q111V individually exhibit monophasic curves suggesting small effects on CG-insensitivity. In contrast, Q111V in combination with A119S (VS/+) results in a right-shifted curve indicating increased CG-insensitivity ($IC_{50,2}$ = 1.6e-6). For VS/+, the 95% CI on the estimated proportion of CG-inhibitable activity of the mutant form, f = 0.54-0.69.

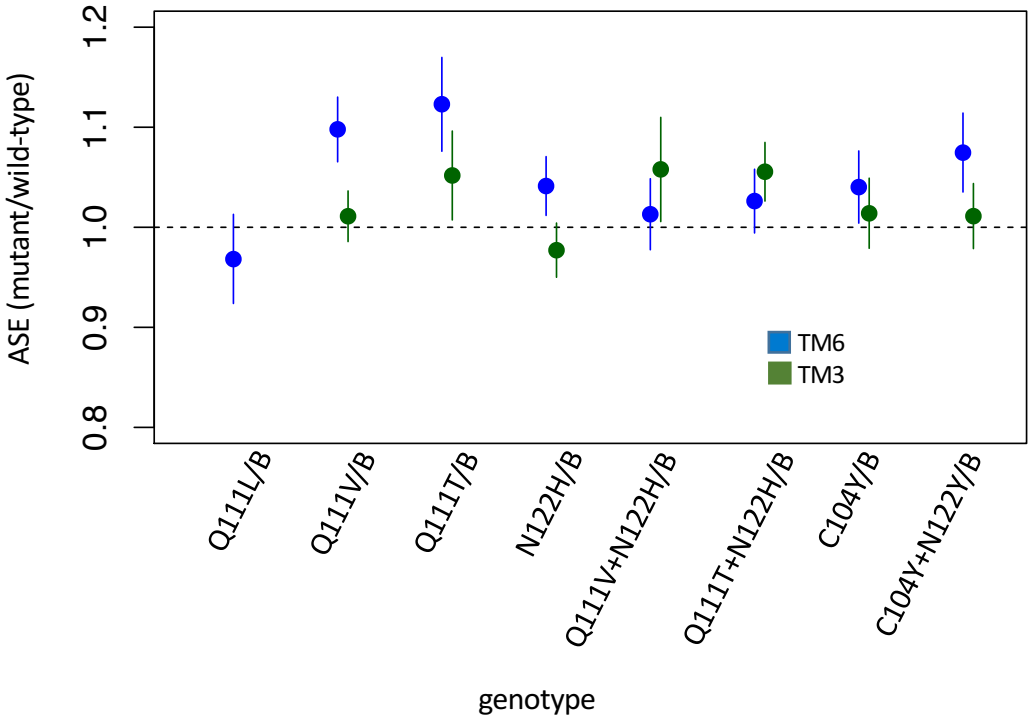

Supplementary Figure S6. Allele-specific expression (ASE) in heterozygous lines. Estimates and 95% confidence intervals are based on Cochran-Mantel-Haenzel framework analysis – i.e. plotted is "relative risk" of the mutant allele in the cDNA population (treatment) using genomic DNA as a control population (see Methods). Equal expression of the two alleles corresponds to a value of 1. Estimates and confidence intervals are shown for alleles balanced over two standard balancer chromosomes, B = TM6 (blue) or TM3 (green) which carries a wild-type allele of ATPα1. While significant deviations from equal expression (correcting for multiple comparisons) are observed for Q111V/TM6, Q111T/TM6, C104Y+N122Y/TM6, Q111T+N122H/TM3, the magnitude of the differences are small and in favor of the mutant allele.

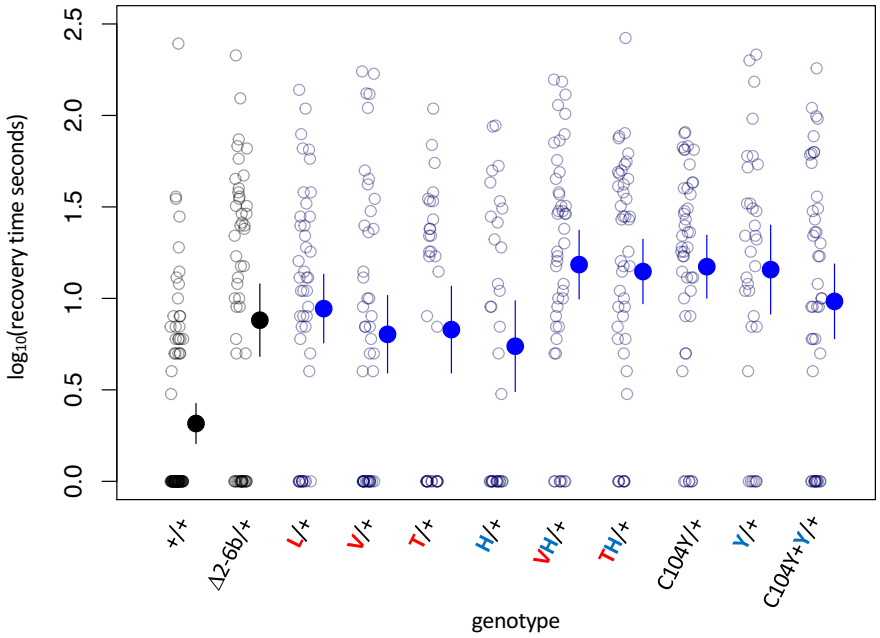

Supplementary Figure S7. Bang sensitivity phenotypes of lines with heterozygous substitutions at sites 104, 111 and 122. Δ2-6b is a loss of function deletion of ATPα1. Red letters indicate substitutions at position 111; blue letters indicate substitutions at position 122. Labels: + = wild-type; Δ2-6b = loss of function deletion of exons 2 through 6b; L = Q111L; V = Q111V; T = Q111T; H = N122H; Y=N122Y. All substitutions are heterozygous over the engineered wild-type allele (+). In all cases, the distributions for substitution lines (Mut/+) are significantly different than the engineered wild-type strain (+/+) ($P < 5e\text{-}5$, Wilcoxon test with continuity correction, correcting for multiple tests).

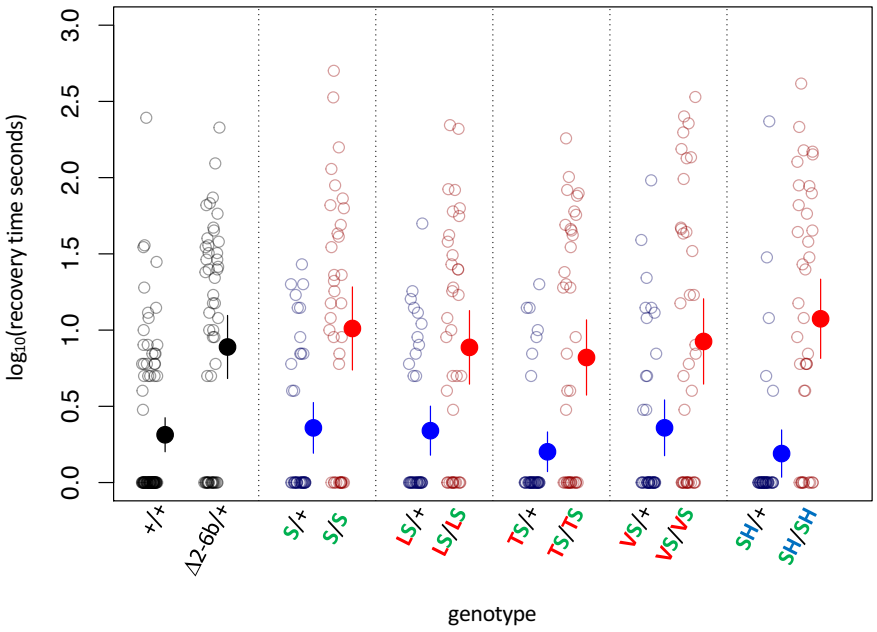

Supplementary Figure S8. Bang sensitivity phenotypes of substitutions at sites 111 and 122 on the background of A119S. Δ2-6b is a loss of function deletion of ATPα1. Red letters indicate substitutions at position 111; green letters at position 119; blue letters at position 122. Blue points and whiskers indicate substitutions that are heterozygous for wild-type allele (+). Red points and whiskers indicate data for homozygous substitutions. Labels: + = engineered wild-type allele; Δ2-6 = loss of function deletion of exons 2-6b; S = A119S; LS = Q111L+A119S; VS = Q111V+A119S; TS = Q111T+A119S; SH = A119S+N122H. In all cases, the distributions for heterozygotes (Mut/+) and homozygotes (Mut/Mut) are significantly different ($P<0.005$, Wilcoxon test with continuity correction, corrected for multiple tests).

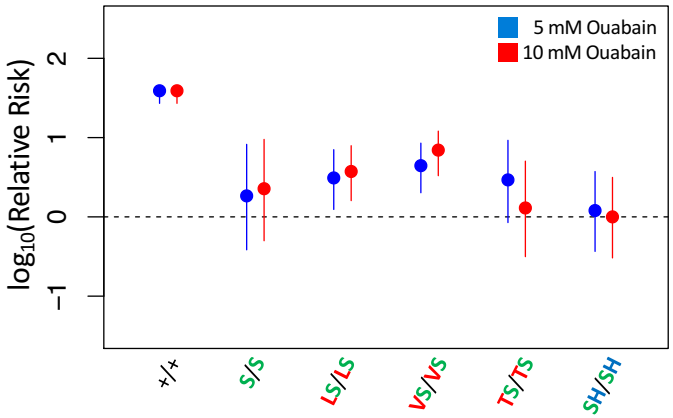

Supplementary Figure S9. Adult survival of homozygous strains with A119S upon 7-day exposure to CGs. Plotted is the log relative risk of treatment, for 5 mM (blue) or 10 mM (red) ouabain, relative to no treatment controls (no ouabain) for homozygous strains. Points and whiskers represent estimates and 95% confidence bounds estimated using the Cochran-Mantel-Haenzel framework (Methods). Each estimate is based in three biological replicates of 20 flies per concentration. A value of 0 corresponds to equal probability of survival of treatment versus control indicating complete insensitivity to the tested ouabain concentration. Labels: +/+ = engineered wild-type strain ; S/S = A119S homozygote; LS/LS = Q111L+A119S homozygote; VS/VS = Q111V+A119S homozygote; TS/TS = Q111T+A119S homozygote; SH/SH = A119S+N122H homozygote.

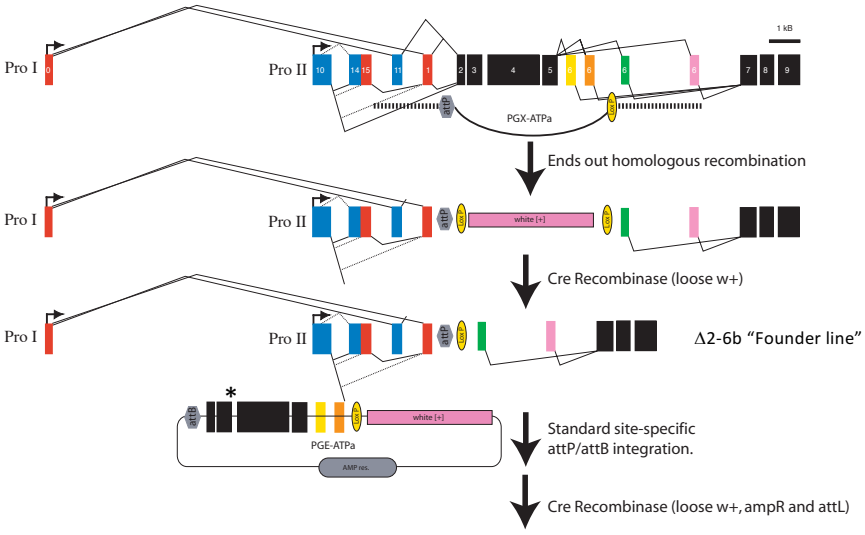

Supplementary Figure S10. Engineering strategy for generating amino acid substitution lines. A targeted replacement of exons 2-6b with a mini-white gene was generated by ends-out homologous recombination. The mini-white gene was removed using cre-lox site-specific recombination to create the Δ2-6b "Founder line". The founder line is injected with the PGE-ATPa plasmid carrying a substitution of choice (asterisk) and incorporated by site-specific phiC31/attP integration. The mini-white gene was removed using cre-lox site-specific recombination to create engineered ATPα (ATPalpha) lines.

Supplementary Table S1. Sources of sequence data used in this study.

Species	Order	Method	Accession	Reference or BioProject
Gryllus firmus	Orthoptera	*RNAseq de novo* assembly	Pending	Yang *et al.* 2019
Tetrix japonica	Orthoptera	*RNAseq de novo* assembly	Pending	Yang *et al.* 2019
Romalea microptera	Orthoptera	*RNAseq de novo* assembly	Pending	Yang *et al.* 2019
Oedaleus asiaticus	Orthoptera	*RNAseq de novo* assembly	Pending	Yang *et al.* 2019
Locusta migratoria	Orthoptera	Sanger cDNA sequencing	KF813097.1	Bao, 2013
Aularches miliaris	Orthoptera	*RNAseq de novo* assembly	MK294065	Yang *et al.* 2019
Taphronota calliparea	Orthoptera	*RNAseq de novo* assembly	MK294066	Yang *et al.* 2019
Dictyophorus griseus	Orthoptera	*RNAseq de novo* assembly	MK294067	Yang *et al.* 2019
Chrotogonus hemipterus	Orthoptera	*RNAseq de novo* assembly	MK294068	Yang *et al.* 2019
Atractomorpha acutipennis	Orthoptera	*RNAseq de novo* assembly	MK294069	Yang *et al.* 2019
Ochrophlebia cafra	Orthoptera	*RNAseq de novo* assembly	MK294070	Yang *et al.* 2019
Sphenarium purpurascens	Orthoptera	*RNAseq de novo* assembly	MK294071	Yang *et al.* 2019
Zonocerus elegans	Orthoptera	*RNAseq de novo* assembly	MK294072	Yang *et al.* 2019
Poekilocerus pictus B	Orthoptera	*RNAseq de novo* assembly	MK294074	Yang *et al.* 2019
Phymateus leprosus B	Orthoptera	*RNAseq de novo* assembly	MK294073	Yang *et al.* 2019
Poekilocerus pictus A	Orthoptera	*RNAseq de novo* assembly	MK294076	Yang *et al.* 2019
Phymateus leprosus A	Orthoptera	*RNAseq de novo* assembly	MK294075	Yang *et al.* 2019
Mantis religiosa	Mantodea	*RNAseq de novo* assembly	Pending	Yang *et al.* 2019
Bemisia tabaci	Hemiptera	Query reference genome	XM_019041063.1	PRJNA352527
Nilaparvata lugens	Hemiptera	Query reference genome	XM_022328639.1	PRJNA398259
Rhodnius prolixus	Hemiptera	Query reference genome	KQ034075.1	PRJNA13648
Lygus hesperus	Hemiptera	*RNAseq de novo* assembly	GBRD01003681.1	PRJNA210219
Cimex lectularius	Hemiptera	Query reference genome	XM_014394884.2	PRJNA298750
Boisea trivittata	Hemiptera	*RNAseq de novo* assembly	JQ771499.1	Zhen *et al.* 2012
Leptocoris trivittatus	Hemiptera	*RNAseq de novo* assembly	JQ771499.1	Zhen *et al.* 2012
Pyrrhocoris apterus	Hemiptera	PCR-sequencing cDNA	HE956739.1	Dobler *et al.* 2012
Dysdercus cingulatus	Hemiptera	*RNAseq de novo* assembly	Pending	SRR5040256
Dysdercus fasciatus	Hemiptera	*RNAseq de novo* assembly	Pending	SRR489295
Macrocheraia grandis	Hemiptera	*RNAseq de novo* assembly	Pending	SRR5040251
Largus californicus	Hemiptera	*RNAseq de novo* assembly	Pending	SRR1821933
Largus sp.	Hemiptera	PCR-sequencing cDNA	HE956738.1	Dobler *et al.* 2012
Jalysus sp.	Hemiptera	*RNAseq de novo* assembly	Pending	SRR1821926
Metatropis rufescens	Hemiptera	*RNAseq de novo* assembly	Pending	SRR2051503
Ischnodemus falicus	Hemiptera	*RNAseq de novo* assembly	Pending	SRR1821925
Gyndes sp.	Hemiptera	*RNAseq de novo* assembly	Pending	SRR5137185
Geocoris sp.	Hemiptera	*RNAseq de novo* assembly	Pending	SRR1821921
Oncopeltus fasciatus D	Hemiptera	*RNAseq de novo* assembly	MK765670	Yang *et al.* 2019
Oncopeltus fasciatus C	Hemiptera	*RNAseq de novo* assembly	JQ771518.1	Zhen *et al.* 2012
Lygaeus kalmii C	Hemiptera	*RNAseq de novo* assembly	JQ771515.1	Zhen *et al.* 2012
Oncopeltus fasciatus B	Hemiptera	*RNAseq de novo* assembly	JQ771519.1	Zhen *et al.* 2012
Lygaeus kalmii B	Hemiptera	*RNAseq de novo* assembly	JQ771514.1	Zhen *et al.* 2012
Oncopeltus fasciatus A	Hemiptera	*RNAseq de novo* assembly	JQ771520.1	Zhen *et al.* 2012
Lygaeus kalmii A	Hemiptera	*RNAseq de novo* assembly	JQ771513.1	Zhen *et al.* 2012
Pediculus humanus corporis	Phthiraptera	Query reference genome	XM_002427669.1	Kirkness et al. 2007
Neodiprion lecontei	Hymenoptera	Query reference genome	XM_015658649.1	PRJNA312506
Athalia rosae	Hymenoptera	Query reference genome	XM_012414228.2	PRJNA282653
Monophadnus latus	Hymenoptera	*RNAseq de novo* assembly	Pending	This study
Pachyprotasis variegata	Hymenoptera	PCR-sequencing cDNA	LN736263.1	Dobler *et al.* 2015
Cephus cinctus	Hymenoptera	Query reference genome	XM_015729628.2	PRJNA297591
Diachasma alloeum	Hymenoptera	Query reference genome	XM_015265214.1	PRJNA306876
Microplitis demolitor	Hymenoptera	Query reference genome	XM_008550885.1	PRJNA251518
Ceratosolen solmsi	Hymenoptera	Query reference genome	XM_011505654.1	PRJNA277475
Copidosoma floridanum	Hymenoptera	Query reference genome	XM_014350407.2	PRJNA297581
Polistes canadensis	Hymenoptera	Query reference genome	XM_014749330.1	PRJNA301748
Polistes dominula	Hymenoptera	Query reference genome	XM_015323700.1	PRJNA307991
Harpegnathos saltator	Hymenoptera	Query reference genome	XM_025304334.1	PRJNA476946
Dinoponera quadriceps	Hymenoptera	Query reference genome	XM_014620740.1	PRJNA301625
Ooceraea biroi	Hymenoptera	Query reference genome	XM_011345351.3	PRJNA501908
Vollenhovia emeryi	Hymenoptera	Query reference genome	XM_012020948.1	PRJNA278668
Pogonomyrmex barbatus	Hymenoptera	Query reference genome	XM_011645049.2	PRJNA276107
Monomorium pharaonis	Hymenoptera	Query reference genome	XM_012678519.2	PRJNA479782
Wasmannia auropunctata	Hymenoptera	Query reference genome	XM_011708535.1	PRJNA279179

Atta cephalotes	Hymenoptera	Query reference genome	XM_012202049.1	PRJNA279976
Acromyrmex echinatior	Hymenoptera	Query reference genome	XM_011052414.1	PRJNA271903
Apis mellifera	Hymenoptera	Query reference genome	XM_020018205.1	PRJNA361278
Apis florea	Hymenoptera	Query reference genome	XM_012490248.1	PRJNA86991
Agrilus planipennis	Coleoptera	Query reference genome	XM_018472182.2	PRJNA343475
Onthophagus taurus	Coleoptera	Query reference genome	XM_023047807.1	PRJNA419349
Tribolium castaneum	Coleoptera	Query reference genome	XM_008198195.2	PRJNA15718
Aethina tumida	Coleoptera	Query reference genome	XM_020018205.1	PRJNA361278
Dendroctonus ponderosae	Coleoptera	Query reference genome	XM_019913697.1	PRJNA360270
Cyrtepistomus castaneus	Coleoptera	*RNAseq de novo* assembly	JQ771502.1	Zhen *et al.* 2012
Hylobius abietis	Coleoptera	*RNAseq de novo* assembly	Pending	SRR6765939
Rhyssomatus lineaticollis A	Coleoptera	*RNAseq de novo* assembly	JQ771524.1	Zhen *et al.* 2012
Rhyssomatus lineaticollis B	Coleoptera	*RNAseq de novo* assembly	JQ771523.1	Zhen *et al.* 2012
Tetraopes tetraophthalmus	Coleoptera	*RNAseq de novo* assembly	JQ771526.1	Zhen *et al.* 2012
Monochamus alternatus	Coleoptera	*RNAseq de novo* assembly	Pending	SRR2521326
Xylotrechus quadripes	Coleoptera	*RNAseq de novo* assembly	Pending	SRR7077078
Megacyllene robiniae	Coleoptera	*RNAseq de novo* assembly	JQ771517.1	Zhen *et al.* 2012
Megacyllene caryae	Coleoptera	*RNAseq de novo* assembly	Pending	SRR1586007
Alticini sp.	Coleoptera	PCR-sequencing cDNA	HE956742.1	Dobler *et al.* 2012
Plagiodera versicolora	Coleoptera	*RNAseq de novo* assembly	JQ771522.1	Zhen *et al.* 2012
Gastrophysa viridula	Coleoptera	PCR-sequencing cDNA	HE956744.1	Dobler *et al.* 2012
Calligrapha philadelphica	Coleoptera	*RNAseq de novo* assembly	Pending	ERR1333730
Labidomera clivicollis	Coleoptera	*RNAseq de novo* assembly	JQ771511.1	Zhen *et al.* 2012
Leptinotarsa decemlineata	Coleoptera	Query reference genome	XM_023161024.1	PRJNA420356
Basilepta melanopus	Coleoptera	*RNAseq de novo* assembly	Pending	SRR8187395
Chrysochus asclepiadeus	Coleoptera	PCR-sequencing cDNA	HE956740.1	Dobler *et al.* 2012
Chrysochus auratus A	Coleoptera	*RNAseq de novo* assembly	JQ771500.1	Zhen *et al.* 2012
Chrysochus cobalitinus A	Coleoptera	*RNAseq de novo* assembly	MK765671	Yang *et al.* 2019
Chrysochus auratus B	Coleoptera	*RNAseq de novo* assembly	JQ771501.1	Zhen *et al.* 2012
Chrysochus cobalitinus B	Coleoptera	*RNAseq de novo* assembly	MK765672	Yang *et al.* 2019
Culex quinquefasciatus	Diptera	Query reference genome	NW_001886804.1	PRJNA29017
Aedes aegypti	Diptera	Query reference genome	NC_035107.1	PRJNA318737
Anopheles gambiae	Diptera	Query reference genome	XM_020076988.1	PRJNA357111
Liriomyza eupatorii	Diptera	PCR-sequencing cDNA	LT795109.1	Petschenka *et al.* 2017
Liriomyza sp.	Diptera	PCR-sequencing cDNA	HE956748.1	Dobler *et al.* 2012
Liriomyza asclepiadis	Diptera	*RNAseq de novo* assembly	MK294077	Yang *et al.* 2019
Chromatomyia horticola	Diptera	PCR-sequencing cDNA	LT795081.1	Petschenka *et al.* 2017
Phytomyza fallaciosa	Diptera	PCR-sequencing cDNA	LT795082.1	Petschenka *et al.* 2017
Phytomyza hellebori A	Diptera	PCR-sequencing cDNA	LT795110.1	Petschenka *et al.* 2017
Phytomyza hellebori B	Diptera	PCR-sequencing cDNA	LT795111.1	Petschenka *et al.* 2017
Phytomyza crassiseta	Diptera	PCR-sequencing cDNA	LT795078.1	Petschenka *et al.* 2017
Phytomyza ilicis	Diptera	PCR-sequencing cDNA	LT795077.1	Petschenka *et al.* 2017
Phytomyza digitalis	Diptera	PCR-sequencing cDNA	LT795083.1	Petschenka *et al.* 2017
Napomyza scrophulariae	Diptera	PCR-sequencing cDNA	LT795080.1	Petschenka *et al.* 2017
Napomyza lateralis	Diptera	PCR-sequencing cDNA	LT795079.1	Petschenka *et al.* 2017
Drosophila mojavensis	Diptera	Query reference genome	XM_015167953.1	PRJNA29977
Drosophila hydei	Diptera	Query reference genome	XM_023321093.1	PRJNA422293
Drosophila virilis	Diptera	Query reference genome	XM_002055964.2	PRJNA29995
Drosophila willistoni	Diptera	Query reference genome	XM_015177397.2	PRJNA29997
Drosophila subobscura QSN	Diptera	*RNAseq de novo* assembly	Pending	This study
Drosophila subobscura QSH	Diptera	PCR-sequencing gDNA	KT318950.1	Pegueroles *et al.* 2016
Drosophila subobscura VSH	Diptera	PCR-sequencing cDNA	KT318946.1	Pegueroles *et al.* 2016
Drosophila guanche	Diptera	Query reference genome	Pending	Puerma et al. 2018
Drosophila obscura	Diptera	Query reference genome	XM_022353228.1	PRJNA399719
Drosophila miranda	Diptera	Query reference genome	XM_017286564.1	PRJNA325520
Drosophila pseudoobscura	Diptera	Query reference genome	XM_001358575.3	Drosophila 12 Genomes Consortium, 2007
Drosophila persimilis	Diptera	Query reference genome	XM_026985943.1	PRJNA501994
Drosophila serrata	Diptera	Query reference genome	XM_020943893.1	PRJNA384652
Drosophila melanogaster	Diptera	Query reference genome	FBgn0002921	ftp://ftp.flybase.net/releases/FB2019_01/
Drosophila simulans	Diptera	Query reference genome	XM_002102615.2	PRJNA297806
Drosophila sechellia	Diptera	Query reference genome	XM_002044256.1	Drosophila 12 Genomes Consortium, 2007
Drosophila erecta	Diptera	Query reference genome	XM_001979324.3	PRJNA501994

Drosophila yakuba	Diptera	Query reference genome	XM_015191921.1	PRJNA29999
Bactrocera cucurbitae	Diptera	Query reference genome	XM_011190816.1	PRJNA273817
Bactrocera oleae	Diptera	Query reference genome	XM_014232491.1	PRJNA293367
Bactrocera latifrons	Diptera	Query reference genome	XM_018929031.1	PRJNA351211
Bactrocera dorsalis	Diptera	Query reference genome	XM_011214825.2	PRJNA273958
Stomoxys calcitrans	Diptera	Query reference genome	XM_013260537.1	PRJNA288986
Musca domestica	Diptera	Query reference genome	XM_020037539.1	PRJNA210139
Lucilia bufonivora	Diptera	PCR-sequencing cDNA	HG938131.1	Mebs *et al*. 2014
Lucilia cuprina	Diptera	Query reference genome	XM_023439570.1	PRJNA423280
Plutella xylostella	Lepidoptera	Query reference genome	XM_011549930.1	PRJNA277936
Saucrobotys futilalis	Lepidoptera	PCR-sequencing cDNA	HE956749.1	Dobler *et al.* 2012
Daphnis nerii	Lepidoptera	*RNAseq de novo* assembly	MK294081	Yang *et al*. 2019
Bombyx mori	Lepidoptera	cDNA sequencing	LC029030.1	Homareda and Hara, unpublished
Empyreuma pugione	Lepidoptera	PCR-sequencing cDNA	LN736266.1	Dobler *et al.* 2015
Olepa ricini	Lepidoptera	*RNAseq de novo* assembly	MK294080	Yang *et al*. 2019
Lerina incarnata	Lepidoptera	PCR-sequencing cDNA	HE956754.1	Dobler *et al.* 2012
Pygoctenucha terminalis	Lepidoptera	PCR-sequencing cDNA	HE956753.1	Dobler *et al.* 2012
Syntomeida epilais	Lepidoptera	*RNAseq de novo* assembly	Pending	This study
Lophocampa caryae	Lepidoptera	*RNAseq de novo* assembly	JQ771510.1	Zhen *et al.* 2012
Euchaetes egle	Lepidoptera	*RNAseq de novo* assembly	JQ771508.1	Zhen *et al.* 2012
Cycnia oregonensis	Lepidoptera	PCR-sequencing cDNA	HE956750.1	Dobler *et al.* 2012
Cycnia tenera	Lepidoptera	*RNAseq de novo* assembly	JQ771504.1	Zhen *et al.* 2012
Trichoplusia ni	Lepidoptera	Query reference genome	XM_026879049.1	PRJNA497582
Trichordestra legitima	Lepidoptera	*RNAseq de novo* assembly	JQ771525.1	Zhen *et al.* 2012
Helicoverpa armigera	Lepidoptera	Query reference genome	XM_021340407.1	PRJNA388211
Bicyclus anynana	Lepidoptera	Query reference genome	XM_024099163.1	PRJNA434100
Vanessa tameamea	Lepidoptera	Query reference genome	XM_026633901.1	PRJNA493654
Limenitis archippus	Lepidoptera	*RNAseq de novo* assembly	JQ771509.1	Zhen *et al.* 2012
Mechanitis polymnia	Lepidoptera	PCR-sequencing cDNA	HF945460.1	Petschenka et al. 2013
Lycorea halia	Lepidoptera	*RNAseq de novo* assembly	JQ771512.1	Zhen *et al.* 2012
Idea leuconoe	Lepidoptera	PCR-sequencing cDNA	HF945457.1	Petschenka et al. 2013
Euploea phaenareta	Lepidoptera	PCR-sequencing cDNA	HF945456.1	Petschenka et al. 2013
Euploea core core	Lepidoptera	*RNAseq de novo* assembly	MK294079	Yang *et al*. 2019
Ideopsis juventa	Lepidoptera	PCR-sequencing cDNA	HF945458.1	Petschenka et al. 2013
Parantica aglea	Lepidoptera	PCR-sequencing cDNA	HF945461.1	Petschenka et al. 2013
Amauris tartarea	Lepidoptera	PCR-sequencing cDNA	HF945450.1	Petschenka et al. 2013
Danaus genutia	Lepidoptera	PCR-sequencing cDNA	HF945453.1	Petschenka et al. 2013
Danaus gilippus	Lepidoptera	*RNAseq de novo* assembly	JQ771506.1	Zhen *et al.* 2012
Danaus chrysippus	Lepidoptera	*RNAseq de novo* assembly	MK294078	Yang *et al*. 2019
Danaus eresimus	Lepidoptera	*RNAseq de novo* assembly	JQ771505.1	Zhen *et al.* 2012
Danaus erippus	Lepidoptera	PCR-sequencing cDNA	HF945451.1	Petschenka et al. 2013
Danaus plexippus	Lepidoptera	*RNAseq de novo* assembly	JQ771507.1	Zhen *et al.* 2012
Tirumala septentrionis	Lepidoptera	PCR-sequencing cDNA	HF945464.1	Petschenka et al. 2013
Tirumala limniace	Lepidoptera	PCR-sequencing cDNA	HF945462.1	Petschenka et al. 2013
Tirumala petiverana	Lepidoptera	PCR-sequencing cDNA	HF945463.1	Petschenka et al. 2013
Pieris rapae	Lepidoptera	Query reference genome	XM_022259192.1	PRJNA397594
Papilio glaucus	Lepidoptera	*RNAseq de novo* assembly	JQ771498.1	Zhen *et al.* 2012
Papilio polytes	Lepidoptera	Query reference genome	XM_013283743.1	PRJNA291535
Papilio machaon	Lepidoptera	Query reference genome	XM_014516575.1	PRJNA300299
Papilio xuthus	Lepidoptera	Query reference genome	XM_013315255.1	PRJNA291600

Supplementary Table S2. References for the phylogenetic relationships of taxa used in this study.

Group	References
Insecta	1
Orthoptera	2–4
Hymenoptera	5–8
Hemiptera	9–12
Coleoptera	13,14
Diptera	15–20
Lepidoptera	21–26

References

1. Misof, B. *et al.* Phylogenomics resolves the timing and pattern of insect evolution. *Science* **346**, 763–767 (2014).
2. Song, H. *et al.* 300 million years of diversification: elucidating the patterns of orthopteran evolution based on comprehensive taxon and gene sampling. *Cladistics* **31**, 621–651 (2015).
3. Song, H., Foquet, B., Mariño-Pérez, R. & Woller, D. A. Phylogeny of locusts and grasshoppers reveals complex evolution of density-dependent phenotypic plasticity. *Sci Rep* **7**, 6606 (2017).
4. Yang, L. *et al.* Predictability in the evolution of Orthopteran cardenolide insensitivity. *bioRxiv* 542811 (2019). doi:10.1101/542811
5. Song, S.-N., Tang, P., Wei, S.-J. & Chen, X.-X. Comparative and phylogenetic analysis of the mitochondrial genomes in basal hymenopterans. *Sci Rep* **6**, 20972 (2016).
6. Boevé, J.-L., Blank, S. M., Meijer, G. & Nyman, T. Invertebrate and avian predators as drivers of chemical defensive strategies in tenthredinid sawflies. *BMC Evol. Biol.* **13**, 198 (2013).
7. Ward, P. S., Brady, S. G., Fisher, B. L. & Schultz, T. R. The evolution of myrmicine ants: phylogeny and biogeography of a hyperdiverse ant clade (Hymenoptera: Formicidae). *Systematic Entomology* **40**, 61–81 (2015).
8. Ward, P. S. The Phylogeny and Evolution of Ants. *Annual Review of Ecology, Evolution, and Systematics* **45**, 23–43 (2014).
9. Yuan, M.-L., Zhang, Q.-L., Guo, Z.-L., Wang, J. & Shen, Y.-Y. Comparative mitogenomic analysis of the superfamily Pentatomoidea (Insecta: Hemiptera: Heteroptera) and phylogenetic implications. *BMC Genomics* **16**, 460 (2015).
10. Li, H. *et al.* Mitochondrial phylogenomics of Hemiptera reveals adaptive innovations driving the diversification of true bugs. *Proc. Biol. Sci.* **284**, (2017).
11. Kikuchi, Y., Hosokawa, T. & Fukatsu, T. An ancient but promiscuous host-symbiont association between Burkholderia gut symbionts and their heteropteran hosts. *ISME J* **5**, 446–460 (2011).
12. Cryan, J. R. & Urban, J. M. Higher-level phylogeny of the insect order Hemiptera: is Auchenorrhyncha really paraphyletic? *Systematic Entomology* **37**, 7–21 (2012).
13. Zhang, S.-Q. *et al.* Evolutionary history of Coleoptera revealed by extensive sampling of genes and species. *Nat Commun* **9**, 205 (2018).
14. Shin, S. *et al.* Phylogenomic Data Yield New and Robust Insights into the Phylogeny and Evolution of Weevils. *Mol. Biol. Evol.* **35**, 823–836 (2018).
15. Junqueira, A. C. M. *et al.* Large-scale mitogenomics enables insights into Schizophora (Diptera) radiation and population diversity. *Sci Rep* **6**, 21762 (2016).

16. Wiegmann, B. M. *et al.* Episodic radiations in the fly tree of life. *Proc. Natl. Acad. Sci. U.S.A.* **108**, 5690–5695 (2011).
17. O'Grady, P. M. & DeSalle, R. Phylogeny of the Genus Drosophila. *Genetics* **209**, 1–25 (2018).
18. Gao, J., Watabe, H., Aotsuka, T., Pang, J. & Zhang, Y. Molecular phylogeny of the Drosophila obscura species group, with emphasis on the Old World species. *BMC Evol. Biol.* **7**, 87 (2007).
19. Williams, K. A., Lamb, J. & Villet, M. H. Phylogenetic radiation of the greenbottle flies (Diptera, Calliphoridae, Luciliinae). *Zookeys* 59–86 (2016). doi:10.3897/zookeys.568.6696
20. Arias-Robledo, G., Stark, T., Wall, R. L. & Stevens, J. R. The toad fly Lucilia bufonivora: its evolutionary status and molecular identification. *Med. Vet. Entomol.* **33**, 131–139 (2019).
21. Zahiri, R. *et al.* A new molecular phylogeny offers hope for a stable family level classification of the Noctuoidea (Lepidoptera). *Zoologica Scripta* **40**, 158–173 (2011).
22. Zahiri, R. *et al.* Molecular phylogenetics of Erebidae (Lepidoptera, Noctuoidea). *Systematic Entomology* **37**, 102–124 (2012).
23. DaCosta, M. A., Larson, P., Donahue, J. P. & Weller, S. J. Phylogeny of Milkweed Tussocks (Arctiidae: Arctiinae: Phaegopterini) and Its Implications for Evolution of Ultrasound Communication. *esaa* **99**, 723–742 (2006).
24. Zenker, M. M. *et al.* Systematics and origin of moths in the subfamily Arctiinae (Lepidoptera, Erebidae) in the Neotropical region. *Zoologica Scripta* **46**, 348–362 (2017).
25. Aardema, M. L. & Andolfatto, P. Phylogenetic incongruence and the evolutionary origins of cardenolide-resistant forms of Na(+) ,K(+) -ATPase in Danaus butterflies. *Evolution* **70**, 1913–1921 (2016).
26. Petschenka, G. *et al.* Stepwise evolution of resistance to toxic cardenolides via genetic substitutions in the Na+/K+ -ATPase of milkweed butterflies (lepidoptera: Danaini). *Evolution* **67**, 2753–2761 (2013).

Supplementary Table S3. Transgenic strains generated in this study.

Line	Substitution(s)	Genotype	M/M viable?	Bang Sensitivity		Ouabain Sensitivity (Adult Exposure)	
				M/+	M/M	M/+	M/M
0	Δ2-6	w^{118};;Δ2-6/TM6	no	yes	.	.	.
1	None	w^{118};;GE-WT	yes	.	ref	.	ref
20	N122H	w^{118};;N122H/TM6	no	yes	.	+++	.
21	Q111L	w^{118};;Q111L/TM6	no	yes	.	+++	.
22	Q111T	w^{118};;Q111T/TM6	no	yes	.	.	.
23	Q111V	w^{118};;Q111V/TM6	no	yes	.	+++	.
24	C104Y	w^{118};;C104Y/TM6	no	yes	.	.	.
25	Q111T,N122H	w^{118};;Q111T, N122H/TM6	no	yes	.	.	.
26	Q111V,N122H	w^{118};; Q111V, N122H/TM6	no	yes	.	.	.
27	C104Y,N122Y	w^{118};;C104Y,N122Y/TM6	no	yes	.	.	.
28	N122Y	w^{118};;N122Y/TM6	no	yes	.	.	.
31	A119S	w^{118};;A119S	yes	no	yes	++	+
32	Q111L,A119S	w^{118};;Q111L,A119S	yes	no	yes	.	+
33	Q111V,A119S	w^{118};;Q111V,A119S	yes	no	yes	+	++
34	A119S,N122H	w^{118};;A119S,N122H	yes	no	yes	+	+
35	Q111T,A119S	w^{118};; Q111T,A119S	yes	no	yes	.	+

NOTE – "TM6" = *TM6B, P{w[+mC]=Dfd-EYFP}3, Sb^1,Tb^1,ca^1*. Δ2-6 is a loss-of-function deletion. M/+ and M/M refer to heterozygous and homozygous substitutions, respectively. Mut/+ were assayed such that the + allele is derived from line 1 (the engineered wild-type strain). "ref" refers to the reference strain used for the assay. "." indicates genotypes that were not assayed. Sensitivity of adults to ouabain exposure is qualitatively scored on a scale from highest = "+++" to lowest = "+".